Quaternary Science Reviews 270 (2021) 107175

Contents lists available at ScienceDirect

Quaternary Science Reviews

journal homepage: www.elsevier.com/locate/quascirev

Anthropogenic and environmental drivers of vegetation change in southeastern Norway during the Holocene

A.T.M. ter Schure [a, *], M. Bajard [b, c], K. Loftsgarden [d], H.I. Høeg [d], E. Ballo [b, c], J. Bakke [e], E.W.N. Støren [e], F. Iversen [d], A. Kool [f], A.K. Brysting [a], K. Krüger [b, c], S. Boessenkool [a, *]

[a] Centre for Ecological and Evolutionary Synthesis, Department of Biosciences, University of Oslo, Oslo, Norway
[b] Department of Geosciences, University of Oslo, Oslo, Norway
[c] Centre for Earth Evolution and Dynamics, University of Oslo, Oslo, Norway
[d] The Museum of Cultural History, University of Oslo, Oslo, Norway
[e] Department of Earth Science and Bjerknes Centre for Climate Research, University of Bergen, Bergen, Norway
[f] Natural History Museum, University of Oslo, Oslo, Norway

ARTICLE INFO

Article history:
Received 19 May 2021
Received in revised form
9 August 2021
Accepted 28 August 2021
Available online xxx

Handling Editor: Yan Zhao

Keywords:
Environmental change
Cultivation
Pastoralism
Lake sediments
Paleolimnology
Archaeology
Scandinavia
Holocene
Metabarcoding
Ancient DNA

ABSTRACT

Uncovering anthropogenic and environmental drivers behind past biological change requires integrated analyses of long-term records from a diversity of disciplines. We applied an interdisciplinary approach exploring effects of human land-use and environmental changes on vegetation dynamics at Lake Ljøgottjern in southeastern Norway during the Holocene. Combined analysis of pollen and sedimentary ancient DNA (*sed*aDNA) metabarcoding of the sedimentary sequence of the lake describes the vegetation dynamics at different scales, and establishes a timeline for pastoral farming activities. We integrate this reconstruction with geochemical analysis of the sediments, climate data, archaeological evidence of local human settlement and regional human population dynamics.

Our data covering the last 10,000 years reveals consistent vegetation signals from pollen and *sed*aDNA indicating periods of deforestation connected to cultivation, matching the archaeological evidence. Multivariate analysis integrating the environmental data from geochemical and archaeological reconstructions with the vegetation composition indicates that the vegetation dynamics at Lake Ljøgottjern were primarily related to natural processes from the base of the core (in ca. 8000 BCE, Mesolithic) up to the Early Iron Age (ca. 500 BCE–550 CE), when agricultural activities in the region intensified. The pollen signal reflects the establishment of a Bronze Age (ca. 1800–500 BCE) farm in the area, while subsequent intensification of pollen concentrations of cultivated plants combined with the first *sed*aDNA signals of cultivation and pastoralism are consistent with evidence of the establishment of farming closer to the lake at around 300 BCE. These signals also correspond to the intensification of agriculture in southeastern Norway in the first centuries of the Early Iron Age. Applying an interdisciplinary approach allows us to reconstruct anthropogenic and environmental dynamics, and untangle effects of human land-use and environmental changes on vegetation dynamics in southeastern Norway during the Holocene.

1. Introduction

Understanding the processes that shaped our modern ecosystems is important for explaining the role of anthropogenic and environmental factors in biological change. It is increasingly recognized that our modern ecosystems are the result of a long history of human-environment interactions (Boivin and Crowther, 2021; Boivin et al., 2016; Ellis, 2015; Ruddiman, 2003; Ruddiman et al., 2015; Williams et al., 2015), with human land-use as one of the major drivers of ecosystem change (Boivin et al., 2016; Ellis, 2015; Nelson et al., 2006; Vitousek et al., 1997). In turn, land-use transitions can be driven by cultural, ecological, and climatic shifts (Boivin et al., 2016; Ellis, 2015; Stephens et al., 2019), illustrating the need for integrated analysis of long-term records from a diversity of disciplines. Here, we combine multi-proxy analysis of

* Corresponding authors. CEES, Dept. of Biosciences, University of Oslo, P.O. Box 1066 Blindern, Europe, NO-0316, Oslo, Norway
E-mail addresses: a.t.m.t.schure@ibv.uio.no (A.T.M. ter Schure), sanne.boessenkool@ibv.uio.no (S. Boessenkool).

https://doi.org/10.1016/j.quascirev.2021.107175

pollen, *sed*aDNA, and geochemical data with knowledge about the local human history as well as palaeodemographic and climatic changes at an inland lake site in southeastern Norway, an area where knowledge on the development of agrarian societies is scarce. We obtain a detailed reconstruction of the palaeoenvironment uncovering the anthropogenic and environmental drivers of biological change.

While in central Europe there were fully developed agrarian societies at around 4000 BCE, Scandinavia by that time was populated by hunter-gatherer-fisher groups and agricultural practices were not adopted until roughly 1500 years later (Bonsall et al., 2002; Krause-Kyora et al., 2013; Price, 2000). Most of what we currently know of the formation of anthropogenic landscapes in Scandinavia comes from pollen analyses and archaeological records, in particular from coastal areas. These records indicate regional differences in timing and rates of the transition from hunter-gatherer-fisher groups to fully developed agrarian societies (Hjelle et al., 2018; Robinson, 2003; Wieckowska-Lüth et al, 2017, 2018), suggesting anthropogenic landscapes were formed through a combination of both rapid introductions by migration processes as well as gradual change within indigenous populations. Ancient mitochondrial DNA analysis of human bones and teeth from coastal areas of Sweden and the Baltic Sea islands suggests Neolithic or post-Neolithic population replacement by migrating farmers (Malmström et al., 2009), possibly driven by improved climatic conditions, allowing agrarian societies from central Europe to migrate northward, introducing crops and agricultural practices (Bonsall et al., 2002; Warden et al., 2017).

Archaeological evidence from Denmark and southern Sweden highlights differences between coastal and inland sites (Sørensen and Karg, 2014), with more rapid introductions of domesticated animals and cereal cultivation in inland sites compared to coastal sites. However, studies on the development of agrarian societies in inland Scandinavia are relatively scarce, possibly because mesolithic settlements were largely shore bound (Solheim and Persson, 2018; Wieckowska-Lüth et al., 2018). Coastal sites are also easier to detect, while bioarchaeological evidence from inland sites is limited, likely due to poorer preservation conditions (Sørensen and Karg, 2014). Within this limited knowledge from inland agrarian shifts, southeastern Norway is particularly underrepresented. Thus far, there are vegetation reconstructions based on pollen from coastal areas in southeastern Norway suggesting small-scale cereal cultivation and animal husbandry in the Early Neolithic (ca. 4000–3300 BCE; Wieckowska-Lüth et al., 2017), crop plant use in the Early Bronze Age (1800 BCE; Soltvedt and Henningsmoen, 2016) and more established cultivation at a later date depending on the region. Long-term settlement of the coastal regions of the Oslo-fjord during the Mesolithic and first part of the Neolithic (8500–2000 BCE; Solheim and Persson, 2018) is evident from archaeological remains and a relatively recent case study from this same region found temporal variation in the use of the coast and the directly adjacent landscape throughout the Mesolithic (ca. 8500–4000 BCE; Wieckowska-Lüth et al., 2018). Pollen analyses of several inland sites in the Romerike region (northeast of Oslo) indicate a delayed introduction of cultivated plants to ca. 2000 BCE following indications of grazing activity from ca. 3000 BCE (Høeg, 1997).

Reconstruction of the extent, intensity, duration and biological consequences of early human land-use requires integrated analyses of long-term records from a diversity of disciplines, combining knowledge about the local human history as well as climatic and other environmental changes. Temporal changes in biological communities can be caused by biological processes such as succession and species dispersal, but these biological changes can be accelerated by environmental factors, e.g. temperature shifts, precipitation, or cultural changes such as through human-mediated introduction of cultivated plants and pastoral animals (Ellis, 2015; Nelson et al., 2006; Vitousek et al., 1997). Identification of the drivers of biological change can be difficult as direct comparison between sites and proxies of environmental change are not always possible, for example due to differences between age-depth models or in spatiotemporal resolution. Detailed multi-proxy reconstructions of the same palaeoenvironmental record are needed to allow comparison and validation of environmental proxies and direct inferences on the timing of environmental changes (Bajard et al., submitted). Lake sediments can be good archives of the palaeoenvironment, integrating biotic and abiotic information across the lake catchment area with temporal stratification. Analysis of pollen and macrofossil remains from lake sediments have previously provided insight in past vegetation and landscape changes, and more recently, sedimentary ancient DNA (*sed*aDNA) analysis has proven valuable for vegetation reconstructions, providing a more local signal and at a higher taxonomic resolution than previously possible (Giguet-Covex et al., 2019; Parducci et al., 2017). Moreover, *sed*aDNA analyses are not limited to the detection of plants and have for instance also been applied to reconstruct pastoral activities (Bajard et al, 2017, 2020; Giguet-Covex et al., 2014) and uncover the effects of these activities, climate change and soil evolution on plant communities (Pansu et al., 2015). By combining pollen analysis with archaeological data, Wieckowska-Lüth et al. (2018) illustrate the value of an integrated approach, allowing the reconstruction of both the intensity and duration of past human land-use. Where archaeological evidence can give insight into societal changes, human settlement patterns and population dynamics, evidence of past presence of cultivated crops, pastoral animals and charcoal can be used to reconstruct a timeline of human presence and land-use changes. Geochemical analysis can further be used to reconstruct past abiotic changes, including physical and chemical weathering, climatic changes and sedimentation processes. Combining these lines of evidence enables identification of periods of biological change, as well as associated abiotic and human land-use changes and their relative timing, thereby allowing inferences about potential driving factors of biological change.

In this study we disentangled anthropogenic and environmental changes on the vegetation dynamics during the last 10,000 years by applying an interdisciplinary approach, focusing on an inland lake site located in southeastern Norway. Lake Ljøgottjern is of particular archaeological interest due to the rich archaeology surrounding the site, including the largest burial mound in Scandinavia: Raknehaugen (Skre, 1997). A new biological reconstruction based on pollen combined with *sed*aDNA metabarcoding describes the vegetation dynamics on different spatial scales, and establishes a timeline for pastoral and arable farming activities. We integrate this reconstruction with geochemical analysis of the same lake sediment record, published climate data and archaeological evidence of local human settlement and regional human population dynamics. Our interdisciplinary approach allows us to reconstruct natural vegetation dynamics during the Holocene, establish a timeline for mixed (pastoral and arable) farming activities, and correlate land-use and environmental changes to vegetation dynamics to uncover human-environment interactions at Lake Ljøgottjern.

2. Regional setting

Lake Ljøgottjern (60°8′54"N, 11°8′18"E, 185 m a.s.l., area: 1.8 hm^2) is located in the middle of the historic Romerike region in southeastern Norway (Fig. 1). It has a maximum depth of 18 m, no inlet or outlet of water, and a small catchment area of 0.15 km^2. Lake Ljøgottjern was formed by a melting block of dead ice after the

retreat of the Scandinavian Ice Sheet ca. 10,000 years ago (Longva and Thoresen, 1989). Sand, gravel and marine clay deposits from the last ice age combined with fluvial deposits from several rivers and the relatively flat geography of the area support the agriculture in the Romerike region. Built on the shore of the lake is the Raknehaugen burial mound, dated to ca. 551 CE (Skre, 1997) and possibly marking the centre of the petty kingdom of Romerike during the Migration Period (ca. 400–570 CE). Raknehaugen is the largest burial mound in Northern Europe at 15 m high, 77 m in diameter, consisting of three substantial layers of timber (pine and birch), with soil and sand from the surroundings. The earliest settlements in this area are dated to the Bronze Age (ca. 1800–500 BCE) and several farmsteads have been located around the lake during the Iron Age (ca. 550 BCE–1050 CE; Helliksen, 1997), while the farmsteads Haug and Ljøgot are known from medieval sources (Rygh, 1898, pp. 322–323), see Fig. 1C. Today, there is still continuous agriculture around Lake Ljøgottjern.

3. Materials and methods

3.1. Sediment coring and sub-sampling

Lake Ljøgottjern was cored at the deepest point in November 2018 (core number LJØ118) and May 2019 (core number LJØ119). The corings were done from a raft using a modified piston corer equipped with a 110 mm diameter, 6 m long PVC tube (Nesje, 1992). Additionally, a 90 mm-Uwitec gravity corer was used to capture the sediment-water interface. The cores were cut into sections of ~140 cm in the field to facilitate transportation and were sealed immediately to reduce the risk of contamination. Cores were preserved in the dark and cold (~4 °C) until opening at the Earth Surface Sediment Laboratory EARTHLAB at the University of Bergen. For each core, one half was used for geochemical analysis, while the other half was used for sediment sampling. Samples for C14 dating were taken from LJØ118, while *sed*aDNA and pollen samples were taken from the LJØ119 and the gravity core. A high sampling and thus temporal resolution was targeted for all analyses as further described below.

Half-cores were sub-sampled at 3 cm intervals for *sed*aDNA immediately upon opening, using 5 mL sterile disposable syringes following the protocol described by Epp et al. (2019). 1 cm^3 subsamples were subsequently collected at 2 cm intervals for pollen and Non Pollen Palynomorphs (NPPs) analyses. *Sed*aDNA samples were transported to the ancient DNA facilities at the University of Oslo and kept at −20 °C until DNA extraction.

3.2. Geochemical analysis and chronology

Both cores were scanned with an ITRAX (XRF) core scanner from COX analytics at the EARTHLAB as described by Bajard et al. (submitted; see also Appendix A.1) with a resolution of 200 μm for LJØ118 and 1000 μm for LJØ119. To obtain matching resolutions of 1 mm and correlate the two cores, Ca, Ti, K, Si, Fe, Mn, Inc and Coh data of LJØ118 were averaged every 5 measures. The depth of the cores were correlated based on the variations in Ti, Fe and Mn and visual observation of the sediment using QAnalyseries 1.4.2 (Kotov and Paelike, 2018). The chronology of the sediment sequence is based on six AMS (accelerator mass spectrometer) radiocarbon dates from plant macrofossils from LJØ118 and realized by the Tandem Laboratory at Uppsala University. The ^{14}C ages were calibrated using the IntCal20 calibration curve (Reimer et al., 2020). The age-depth model for the LJØ118 sequence was generated using R software (version 3.5.2; R Core Team, 2020) and the R code package 'Bacon' 2.4.3 (Blaauw and Christen, 2011). In the age model, the top of the core was set to the year of coring, i.e. 2018 CE. The chronology of LJØ119 was deduced from the LJØ118 age model.

XRF measurements of Ti were used as a proxy for terrestrial sediment influx into the lake, while the Inc/Coh ratio was used to

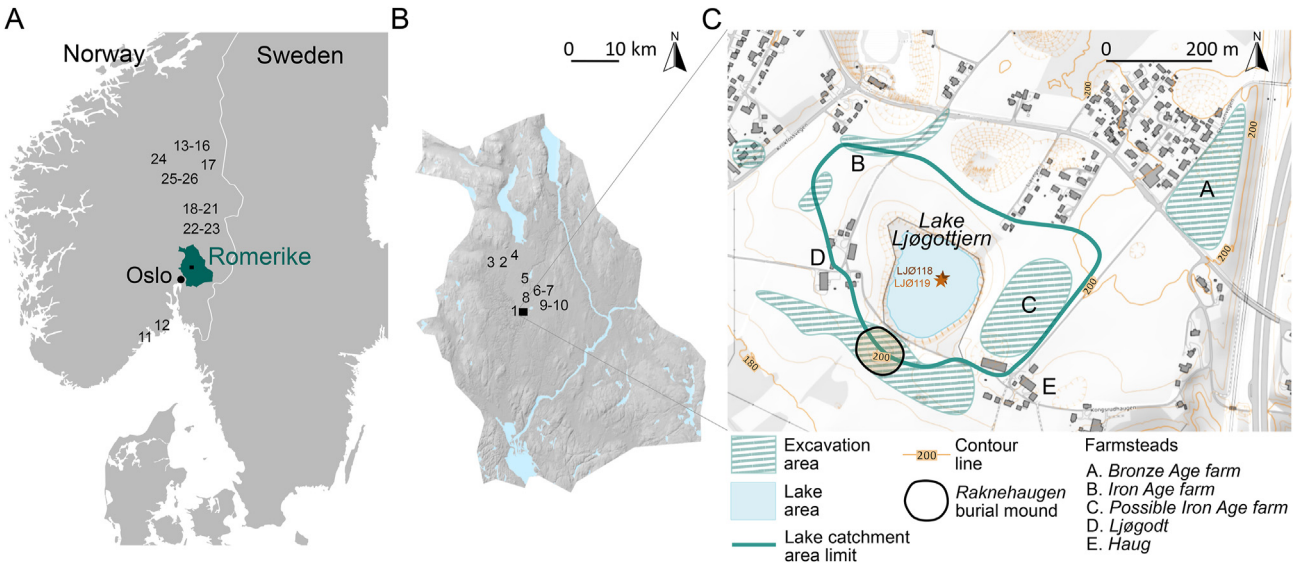

Fig. 1. Location of the areas under study, with the historic Romerike region in southeastern Norway (A), Lake Ljøgottjern in the historic Romerike region (B), and a topographic map of the area surrounding Lake Ljøgottjern from www.kartverket.no (C), including the lake catchment area indicated with a solid blue line, stars indicating the location of the sediment cores in the lake, contour lines in solid orange, archaeological excavation areas indicated with hatching, and farmsteads of interest indicated with capital letters. Raknehaugen is a burial mound dated to ca. 550 CE (Skre, 1997) and indicated here with a black circle. Numbers in (A) and (B) indicate locations of pollen records mentioned in the text and correspond to: 1. Lake Ljøgottjern, described in this study, 2. Rud Øde, 3. Bjørkemosan, 4. Lybekkmosan, 5. Danielsetermyr, 6. Bånntjern in Ullensaker, 7. Svenskestutjern, 8. Skånetjern, 9. Myr ved Pinnebekk, 10. Myr ved Brenni, described by Høeg (1997); 11. Skogstjern, described by Wieckowska-Lüth et al. (2017); 12. Nordbytjern, described by Soltvedt and Henningsmoen (2016); 13. Bånntjern in Tolga, 14. Stortallsjøen, 15. Lensmannsvollen, 16. Kåsmyra, 17. Lille Sølensjøen, 18. Ottersmyra, 19. Dulpmoen, 20. Ulvehammeren, 21. Kilde, 22. Engelaug, 23. Hellemundsmyra, 24. Grimsdalen, 25. Skjerdingsfjell, and 26. Hirsjøen, described by Høeg (1996). (For interpretation of the references to colour in this figure legend, the reader is referred to the Web version of this article.)

estimate changes in the organic matter content of the lake sediment. Peaks of Ti can reflect erosion events such as heavy rainfall and floods (Bajard et al., submitted), or human activities (Arnaud et al., 2016; Bajard et al., 2016). To facilitate statistical analyses, time resolutions of the Ti measurements and Inc/Coh ratio were matched to the resolution of the vegetational datasets from the pollen and the *sed*aDNA analyses using generalised additive models (GAM; Appendix A.1).

3.3. Pollen and charcoal analyses

We prepared 131 sediment sub-samples of 1 cm^3 as described in Faegri et al. (1989). For the period between 200 and 1250 CE, pollen samples were analysed in timesteps of ~18 years (every 1–2 cm) while timesteps were longer for the rest of the period covered by the core (30–300 years; 3–40 cm). Tablets of spores (*Lycopodium clavatum*) were added to each sample to calculate pollen and charcoal concentrations (Stockmarr, 1971). At least 500 pollen grains of terrestrial plants were identified and counted in each sample. Further analyses are based on pollen concentrations to allow comparison to the *sed*aDNA data, as both estimates are standardized to a fixed amount of sediment. Pollen terrestrial plant diversity was determined by Hill numbers with the *hill_taxa* function of the *HillR* R package (Li, 2018; R Core Team, 2020), where $q = 0, 1$ and 2 were used to obtain the number of identified pollen types, Shannon index and inverse Simpson index. Charcoal preserved in the lake sediments can be used as an indicator of human presence. To include charcoal in further statistical analyses we matched the calibrated ages of the samples and the *sed*aDNA dataset using linear interpolation.

3.4. DNA analyses

3.4.1. DNA extraction and amplification

We extracted DNA from 40 samples covering timesteps of ~80 years for the period 200–1800 CE (approx. every 9 cm) and timesteps of around 450–500 years in the rest of the period covered by the core. Six extraction negative controls were included and DNA was extracted using the PowerSoil DNA Isolation Kit (Qiagen) following manufacturers' protocol with two modifications: extracts were lysed overnight leaving the PowerBead Tubes with C1 solution at 37 °C for 16–20 h under constant rotation (Epp et al., 2019), and eluted in 100 μL elution buffer supplied with the kit. DNA extraction, PCR preparation and post-PCR work were carried out at the ancient DNA lab facilities of the University of Oslo.

Plant DNA was amplified using the *trn*L *g* and *h* primers that amplify the P6 loop of the *trn*L intron (Taberlet et al., 2007), while mammal DNA was amplified using the Mam-P007 primers (Giguet-Covex et al., 2014). Forward and reverse primers were tagged with a unique 8 or 9 bp barcode at the 5' end to allow for multiplexing as described by Voldstad et al. (2020), with each primer pair having the same tag. Six individually tagged PCR replicates were prepared for each sample and primer set and at least one PCR negative control was included per 12 replicates. Plant DNA amplifications were carried out following Alsos et al. (2016), halving the total reaction volume to 25 μL, but keeping the same volume of bovine serum albumin (8 μg; BSA, Roche Diagnostic, Basel, Switzerland) and DNA (5 μL). Mammal DNA amplifications were carried out in the same amplification mixture as for the plants, with the addition of human blocker (Boessenkool et al., 2012) at a concentration of 2 μM to restrict amplification of human DNA when amplifying mammalian DNA. Both the plant and mammal PCR mixtures were denatured at 95 °C for 10 min, followed by 45 cycles of 30 s at 95 °C, 30 s at 50 °C, 1 min at 72 °C and a 10 min final elongation at 72 °C.

We evaluated amplification success by gel electrophoresis before equivolume pooling of PCR products based on PCR band strength (including those that showed no band) to a maximum volume of 500 μL and cleaned using MinElute Purification kit (Qiagen) following manufacturers' instructions. Concentrations of the cleaned products were measured on a Qubit 2.0 with the Qubit dsDNA HS kit (ThermoFisher). Purified products were then pooled before sequencing, while preventing overlap in demultiplex-tags, resulting in two pools (of 320 and 298 PCR replicates). Libraries were built from the two pools using the KAPA HyperPrep DNA kit (Roche) with Illumina Unique Dual Indexes and these were sequenced on separate lanes on the Illumina HiSeq 4000 platform (2 × 150-bp, paired-end) at the Norwegian Sequencing Centre.

3.4.2. DNA sequence analyses and filtering

We processed the *sed*aDNA sequence data using the OBITools package (https://metabarcoding.org/obitools/doc/index.html; Boyer et al., 2016). Assembling the forward and corresponding reverse reads was done using *illuminapairedend*, followed by sample assignment with *ngsfilter*. We removed reads with a quality score <40, <100% tag match, >3 mismatches with the primers, shorter lengths then expected (<8 bp), with a sequence that is present exactly once, and those containing ambiguous nucleotides. Amplification and sequencing errors were identified using *obiclean*, with a threshold ratio of 5% for reclassification of sequences identified as 'internal' to their corresponding 'head' sequence. Sequences that were identified only as 'internal' were removed. Finally, sequences were compared to their relevant taxonomic reference libraries using *ecotag*. The reference libraries were prepared by performing an in-silico PCR with the *ecoPCR* software (Ficetola et al., 2010) using the NCBI Taxonomy database (https://www.ncbi.nlm.nih.gov/taxonomy).

For the plant identifications, we used two reference libraries. The first reference library (arctborbryo) contains 2289 unique sequences, with 815 Arctic (Sønstebø et al., 2010), and 835 boreal (Willerslev et al., 2014) vascular plant taxa and 455 bryophytes (Soininen et al., 2015). To mitigate erroneous or missing taxonomic assignments due to lacking references in the first library, we prepared a second reference library based on the global EMBL database (release 142, January 2020), containing 19,533 unique sequences from 14,327 plant taxa. Also for the mammal identifications we prepared a reference library based on the global EMBL database (release 142, January 2020), containing 41,257 unique sequences from 24,068 mammal taxa.

In order to minimise any misidentifications, we filtered the identified sequences in R (version 3.5.2; R Core Team, 2020) using similar requirements as Alsos et al. (2018) removing (1) sequences with higher occurrence (i.e. more reads): in negative controls than in samples, (2) sequences with a <100% (plants) or <98% (mammals) match, (3) sequences with <10 reads in a PCR replicate (plants) or in the total dataset (mammals), (4) PCR replicates with <100 reads in total, (5) sequences present in <2 PCR replicates of a sample, and (6) sequences with a mean read count >mean read count in the negative controls. In order to check and where possible narrow down some of the taxonomic identifications, the identified plant taxa were checked by botanists with extensive knowledge of the local flora. For the mammal dataset we removed genera that are not of interest for this study. Remaining unique sequences were designated as molecular operational taxonomic units (MOTUs). An overview of the filtering steps and their effect on the size of the dataset can be found in Appendix Table A.2.

To correct for the exponential increase in read counts during PCR, we log-transformed the filtered plant and mammal MOTU datasets (Giguet-Covex et al., 2019) and calculated relative read abundances (RRAs) to further facilitate comparison between samples. Both plant and mammal datasets were reduced by merging

the PCR replicates, while calculating the number of positive replicates per MOTU and the mean RRA values. We assessed the quality of the samples by computing the summed read counts and the average read counts (+-SE; Appendix A.3). No significant relationship between summed or average read counts and the plant biodiversity estimates per replicate or per sample was found (Appendix A.4), indicating absence of a potential bias in biodiversity estimates due to differences in sample size. We found significant correlations between the number of positive replicates and the transformed read counts per MOTU (Appendix A.5) and based subsequent analyses on the more conservative positive replicates.

Terrestrial plant diversity was determined by Hill numbers with the *hill_taxa* function of the *HillR* R package (Li, 2018), using q = 0, 1, and 2 to obtain the number of MOTUs, Shannon index and inverse Simpson index (Chao et al., 2014). The presence of DNA from livestock represents a proxy for pastoralism and we include presence/absence of livestock DNA in subsequent statistical analyses.

3.5. Palaeodemographic analysis

Radiocarbon dates from archaeological sites can be used as a proxy to estimate of the past population densities, accepting the basic premise of a relationship between quantities of radiocarbon dates and intensity of past population or activity (Freeman et al., 2018; Rick, 1987; Solheim and Iversen, 2019; Loftsgarden and Solheim, in press).

We analysed 476 radiocarbon dates from archaeological contexts in the Romerike region using Summed Probability Distribution (SPD) analysis within the *rcarbon* package (Crema and Bevan, 2021). Dates were calibrated using the Intcal20 calibration curve (Reimer et al., 2020). The use of SPDs allows us to study long-term developments on a spatial and temporal level. The obtained SPDs were subsequently matched to the calibrated ages of the pollen and DNA samples to facilitate statistical comparison.

3.6. Climate data

We obtained published multi-proxy surface temperature anomaly composites from the northern hemisphere (Kaufman et al., 2020) and the North Atlantic-Fennoscandian region (Sejrup et al., 2016), with proxies including oxygen isotopes, alkenone biomarkers, assemblages of pollen, chironomids, and diatoms among others. The Sejrup et al. (2016) temperature anomaly reconstruction composite is based on 81 proxy derived surface and near-surface summer temperature time series from 74 lake and marine sites in the North Atlantic and Fennoscandia (40E–40W, 58–80N) spanning the last 10,000 years. Kaufman et al. (2020) present a multi-method 100 year time-step reconstruction of global mean surface temperatures of the last 12,000 years based on the temperature 12 k database of palaeo-temperature time series. From this publication we included the median values of the 60–90 N northern hemisphere temperature composite.

General Additive Models (GAMs) allow flexible modelling of nonlinear relationships (Simpson, 2018), and were fitted to the temperature data using the *gam* function in the *mgcv* R package (Wood, 2018) to smooth and interpolate values and match the time resolutions of the pollen and DNA datasets. Further statistical analyses were performed with temperature data from both the Kaufman et al. (2020) and the Sejrup et al. (2016) data, but as results were similar we only present results including the Sejrup et al. (2016) data in the main text and figures (see Appendix A.6 for results including the Kaufman et al., 2020, data).

3.7. Statistical analyses

All statistical analyses were performed in R. To summarize the vegetation data, pollen and plant DNA taxa were assigned to one of 10 plant groups: anthropochores, apophytes, forbs, graminoids, aquatics, bryophytes, clubmosses, ferns, shrubs, trees, and remaining taxa were grouped to “other” (Appendices B.1–3). To visualize changes in abundance of plant taxa over time (i.e. pollen concentrations, number of positive DNA replicates) and mammal genera, we created stratigraphic plots with the *rioja* package (Juggins and Juggins, 2020; Appendices A.7–8). This package was also used for stratigraphically constrained cluster analysis using the CONISS algorithm (Grimm, 1987), identifying zones of similar terrestrial plant community composition (see Appendix A.9 for details). For a visual summary of the changes in abundance of plant groups over time, we calculated pollen fractions and DNA replicate fractions by summing the pollen concentrations and positive DNA replicates per plant group and dividing this by the total sum. To obtain estimates of the accumulation rate of taxa per plant group, we calculated the cumulative numbers of MOTUs and pollen types using the *specaccum* function of the *vegan* package (Oksanen et al., 2020).

To investigate plant community trajectories we used non-metric multidimensional scaling (NMDS), and to test how plant community trajectories relate to environmental change we applied a stepwise distance-based redundancy analysis (dbRDA) based on Bray-Curtis dissimilarities of Hellinger-transformed data. Where NMDS allows analysis of the total variation in the plant taxonomic composition, it is less suited for fitting environmental variables than dbRDA. The latter was specifically developed to test the significance of relationships between environmental variables and biological response data (Legendre and Anderson, 1999), but only analyses the variation explained by the environmental terms (Ramette, 2007). The environmental terms (i.e. Ti, Inc/Coh ratio, charcoal, presence/absence of livestock, ^{14}C SPD, temperature anomaly) were standardized with the *decostand* function, removing unwanted effects of different measurement units. For the dbRDA, we performed automatic stepwise model building combining the *ordiR2step* and *capscale* functions to obtain the best fitting model. We subsequently tested for statistical significance ($p < 0.05$) of the included environmental terms with an anova (999 permutations) and calculated the proportion of plant community variance explained by each term in the model. We also performed variation partitioning using the *varpart* function for assessing joint effects of the environmental terms included in the dbRDA model. Spearman's rank correlation coefficient was used to identify relationships between environmental terms and we applied the bonferroni method to correct *p*-values for multiple comparisons. For further details on these steps, see Appendices A.10–12.

3.8. Archaeological evidence

We collected and analysed existing archaeological and historical evidence on settlements and land-use around Lake Ljøgottjern. We used the *Askeladden* database of Norwegian archaeological sites and monuments (https://askeladden.ra.no/; hosted by the Directorate for Cultural Heritage, 2020) and the *UniMus* database of archaeological artefacts and samples (http://unimus.no; Universitetsmuseenes samlingsportaler, 2020). Further information on pre-modern farmsteads and farm territories around Lake Ljøgottjern was obtained from the standard works of *Norske Gaardnavne* (https://www.dokpro.uio.no/rygh_ng/rygh_felt.html), *Diplomatarium Norvegicum* (https://www.dokpro.uio.no/dipl_norv/diplom_felt.html) and public available enclosure maps dated 1890 and 1902 (https://wcarkiv.domstol.no/wcarkiv/kommunelist.wc?

ID). This was further supplemented with information from literature on local history (Hagen, 1997, pp. 28–30; Johnsen, 1941, pp. 133–134; Nesten, 1951).

4. Results

4.1. Description of the sediment

4.1.1. Lithology and geochemistry

Ten different lithological facies were identified for the 535 cm of sediment of the Lake Ljøgottjern sediment sequence (Fig. 2). The bottom part (535–440 cm) presents fine regular light and dark laminations (<1 mm). From 440 to 391 cm depth, the sediments are disturbed and oblique levels were found in LJØ118. This part of the sediment is also disturbed in LJØ119 with folded features. This section can be interpreted as a slump and outside of the continuous sedimentation. It was considered as an instantaneous deposit and removed from the age-depth modelling. Above this deposit, the sediment is composed of dark organic silt with layering until 350 cm. Below 350 cm, Fe intensities are high (123 kcps average) and show variability (s = 44 kcps). Above 350 cm, the dark organic silt does not present layering anymore and Fe declines suddenly, remaining close to 0 kcps until 280 cm, while the Inc/Coh ratio reaches a maximum in this facies. For the whole sequence, intensities of Ti and K are very similar. Below 280 cm, K and Ti are very low (close to 0 cps) except several synchronous high peaks. Above 280 cm, intensities of K and Ti are higher (averaging at 170 and 230 cps) and represent the main change in the sedimentation of the sequence. Fe increases again and the Inc/Coh ratio remains at a high level. The following facies present dark organic silt with orange level or thin laminations. The two uppermost facies are coarse silt and present several layers of different colors. Peaks of Ti and K in the top part of the sequence were related to historical floods as identified by Bajard et al. (submitted). See Appendix A.1 for an overview of all XRF results.

4.1.2. Chronology

The age-depth model of the sediment sequence is constrained by six ^{14}C-dated plant macrofossil samples. Details of the samples and calibrated ages are presented in Appendix Table A.1. The top part was set to the year of coring and verified with the deposit of the historical flood "Stor-ofsen" of 1789 (Bajard et al., submitted). The resulting age-model covers the last 9300 years (Fig. 2). The top part of the age-model is linear until 250 cm with a mean sedimentation rate of 1.25 mm. yr-1. There is a shift in the sedimentation rate between 250 cm (50 cal CE) and 375 cm (5350 cal BCE), which was set at 280 cm (350 cal BCE) in the age-model considering the major change in the lithology and geochemistry at this depth. The sedimentation rate of the 5350–350 cal BCE period is much lower, ca. 0.2 mm. yr-1. The instantaneous deposit identified in section 4.1.1 is dated to 5650 cal BCE. Below this deposit, the laminated sediment covers the period 7350–5650 cal BCE with a sedimentation rate of 0.5 mm. yr-1 in average.

4.2. Description of the biological data

4.2.1. Pollen

A total of 110 pollen types were counted in the pollen analysis, of which 65 plant families, 88 genera, and 12 species were identified. Pollen concentrations in samples from the instantaneous deposit were averaged to one concentration per pollen type, reducing the number of samples from 131 to 121. The most abundant plant groups in the pollen concentration dataset were trees (65%), followed by aquatics (17%), graminoids (7%) and anthropochores at 4% (Fig. 3A). The most abundant families were tree families Betulaceae (33%) and Pinaceae (28%), followed by green algae (Botryococcaceae) at 12%. Detailed pollen concentration diagrams can be found in Appendix Fig. A.7 and the corresponding data in Appendix Table B.1.

4.2.2. Plant and mammal DNA

For the first and second sequencing pools we obtained a total of

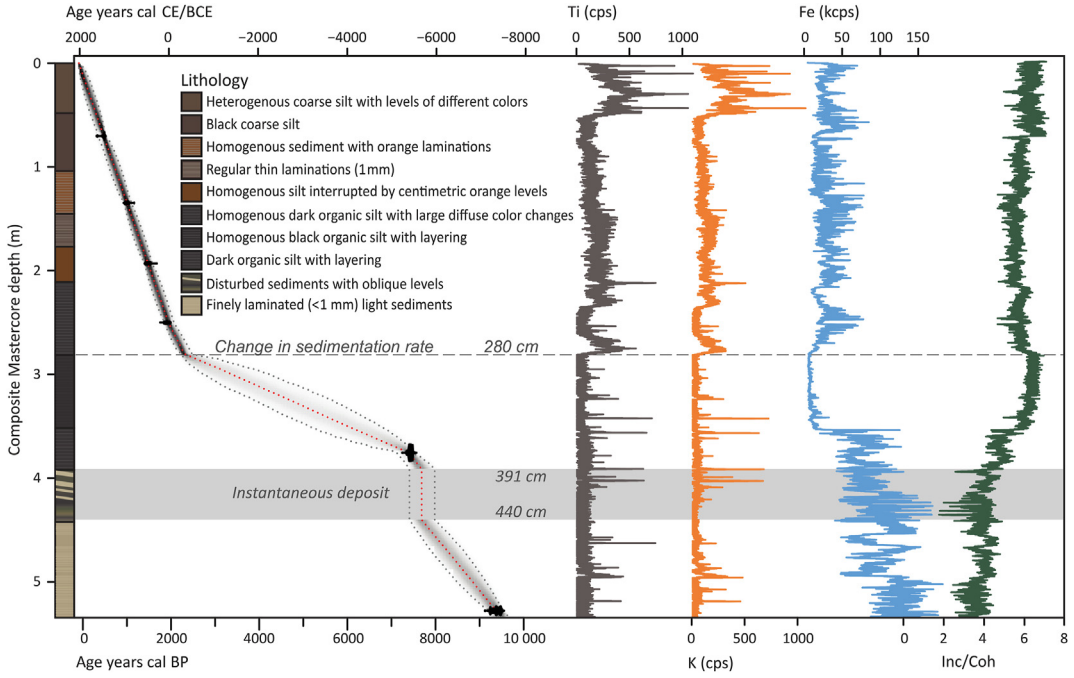

Fig. 2. Age-depth model of the Lake Ljøgottjern sediment sequence (as represented with Bacon R package), including lithology and XRF geochemistry (Ti, K, Fe and Inc/Coh in counts per second). A change in the sedimentation rate was set at a depth of 280 cm based on the change in sediment and XRF geochemistry. We identified an instantaneous deposit of sediment at 391–440 cm depth.

220,591,834 and 64,492,511 reads, respectively. After filtering, the plant DNA dataset consisted of 34,300,823 reads with on average 151,425 ± 20,349 reads per sample, corresponding to a total of 274 unique MOTUs (Fig. 3A, Appendix A.2–3). Taxonomic assignments of the plant sequences allowed us to identify 74 different plant families, 136 genera and 86 species (Appendices B.2–3).

The largest plant groups in relative log transformed read abundances were aquatic plants (37%), followed by forbs (non-graminoid herbaceous plants; 28%) and trees (20%). The same plant groups dominated when analysing the summed number of positive replicates, with the largest contribution from forbs (3978, 45%), followed by aquatic plants (1918, 22%) and trees (1191, 13%) (33%, 30% and 20%, respectively, when fractionated per sample as in Fig. 3A).

For the mammal DNA we obtained a total of 24,287,943 reads after filtering, corresponding to 119 unique MOTUs, from 3 different families and 5 genera, namely cattle (*Bos* sp.; 78 MOTUs), horses (*Equus* sp.; 11 MOTUs), pigs (*Sus* sp.; 1 MOTU), goats (*Capra* sp.; 3 MOTUs), and sheep (*Ovis* sp.; 26 MOTUs). Plant DNA was detected throughout the sediment core, while mammal DNA was only found in samples dating from ~200 BCE to 1800 CE. The number of read counts per sample in this time period averaged to 196,876 ± 60,890 (Appendices A.3 and B.4–5).

4.3. Plant identification by pollen versus sedaDNA

*Sed*aDNA detected a higher number of plant taxa and more taxa at a higher taxonomic level than was achieved by pollen. Of all detected plant families, 48 were detected by both methods, while 17 were unique to the pollen and 26 to the *sed*aDNA dataset, most of which were forbs (10), bryophytes (7) and aquatic plants (4), while plant families unique to the pollen dataset were primarily forbs (4), aquatics (4) and shrubs (3). Regarding plant genera, 52 were shared compared to 36 unique genera to the pollen dataset and 84 to the *sed*aDNA dataset. For the anthropochore and apophyte plant groups, containing mainly cultivated plant taxa and those benefiting from human disturbance, in total 17 pollen types were recorded compared to 15 MOTUs. For example, *Secale* was identified among the pollen but not detected by the *sed*aDNA despite its presence in the used reference database. *Sed*aDNA was able to identify both *Hordeum* and *Avena* as well as *Cannabis* and *Humulus*, while these pairs could not be distinguished from their pollen. For the forbs, 34 pollen types were recorded compared to 152 MOTUs from 21 to 31 plant families, respectively (Appendices B.1–3).

4.4. Plant community dynamics

4.4.1. Terrestrial vegetation zones

Two separate zones of similar terrestrial plant community composition were identified based on the plant *sed*aDNA dataset using CONISS clustering analysis, with the boundary between 580 and 230 cal BCE. Analysis of the pollen dataset identified 4 additional zones, though the broken stick analysis showed minor differences when adding the 3 last identified zones (Appendix Fig. A.9). Consequently, we identified one additional zone based on the pollen dataset, with the boundary between 440 and 450 CE. With the higher resolution of the pollen samples, the previously identified *sed*aDNA based zone was further delineated to between 430 and 320 cal BCE (Fig. 3B). NMDS ordination of pollen and *sed*aDNA data supported the results of the CONISS clustering analysis (Appendix Fig. A.10).

4.4.2. Vegetation zone 1 (ca. 8000–300 cal BCE)

Between 8000 and 7000 cal BCE, a relatively high rate of accumulation of new taxa was found, as cumulative numbers increased from 18 to 44 for the pollen and 9 to 40 for the plant DNA (Fig. 3A). Terrestrial plant biodiversity remained low throughout the 8000–300 cal BCE period with estimates <10 for pollen and <22 for the DNA MOTUs, averaging to 5.0 ± 0.2 ($q = 1$) and 3.4 ± 0.2 ($q = 2$) for pollen, and 11.4 ± 1.5 ($q = 1$) and 10.7 ± 1.4 ($q = 2$) for *sed*aDNA (Fig. 3B).

From 8000 to 3100 cal BCE, both the pollen and *sed*aDNA records were dominated by trees (93% and 64%). Recorded pollen types included *Betula* (52%), *Pinus* (24%), *Alnus* (12%), *Corylus* (5%), *Ulmus* (3%), and 3% of *Tilia*, *Quercus, Populus, Fraxinus* and *Fagus* combined. Pollen concentrations of shrubs were relatively stable, with an average of <1% of the terrestrial pollen concentration, and higher percentages (~2%) in the period between 7500 and 7000 cal BCE. *Sed*aDNA trends for shrubs were more variable, with percentages often at 0, but also peaking to 10, 17 and 43% at 7500, 2000 and 1600 cal BCE. At 2800 cal BCE, a distinct peak was found in the concentration of graminoid pollen, while in the DNA data a peak in graminoids was recorded later, at 2100 cal BCE. Forbs (<1% pollen, 15% DNA) and ferns (1% pollen, 9% DNA) were recorded throughout zone 1. No DNA of plants commonly associated with human settlements (apophytes and anthropochores) was found, while traces of pollen of these groups were found throughout this zone (<2%).

4.4.3. Vegetation zone 2 (ca. 300 cal BCE–450 cal CE)

A period of rapid increase in cumulative numbers of taxa could be distinguished between ca. 300 cal BCE and 450 cal CE for both pollen and *sed*aDNA records, as cumulative pollen types increased from 67 to 101, plant DNA MOTUs from 81 to 224 (Fig. 3A) and biodiversity estimates increased to averages of 8.1 ± 0.3 ($q = 1$) and 4.9 ± 0.2 ($q = 2$) for pollen, and 82.4 ± 16.4 ($q = 1$) and 78.0 ± 15.8 ($q = 2$) for *sed*aDNA (Fig. 3B).

We detected a reduction in tree pollen to 79% of the total pollen concentrations, and an increase in average abundance of mainly graminoids in the pollen record (from <1% to 9%) and forbs in the DNA record (from 15% to 62%). Concentrations of graminoid pollen fluctuated around 10% of the terrestrial pollen concentration, with notable reductions to below 5% at ~250 cal BCE and 450 cal CE, while graminoids in the *sed*aDNA record decreased in number of positive replicates throughout this zone, from 10% to 2%.

After 300 cal BCE, anthropochore and apophyte taxa first appeared in the *sed*aDNA record, simultaneously with increased abundances in the pollen record from 1.5% to 2% (apophytes) and 0.4%–2.4% (anthropochores) and an increase in graminoids from <5% to >13% at 250 cal BCE. A decrease in relative pollen concentrations of apophytes and anthropochores was recorded at around 50 cal BCE, after which both groups returned to previous percentages, reaching 5% around 350 cal CE (apophytes) and 11% at ca. 450 cal CE (anthropochores).

4.4.4. Vegetation zone 3 (ca. 450–1800 cal CE)

Biodiversity increased to averages of 10.0 ± 0.3 ($q = 1$) and 5.8 ± 0.2 ($q = 2$) based on the pollen data, while estimates based on *sed*aDNA data decreased to 61.5 ± 5.3 ($q = 1$) and 58.1 ± 5.0 ($q = 2$) compared to the previous zone. Cumulative numbers of taxa increased until 1600 cal CE for the pollen, and 1800 cal CE for the plant *sed*aDNA (Fig. 3B).

Tree pollen concentrations continued to decrease until ~1300 cal CE, while still dominating the pollen record at an average of 68% of the terrestrial pollen concentration. In the *sed*aDNA record, trees averaged at 14% with some fluctuation, while forbs remained dominant at an average of 62% for this zone. The *sed*aDNA relative fractions of shrubs peaked at 1200, 1400 and 1600 cal CE, and pollen concentrations similarly indicate increased abundance of shrubs around 1200 and 1400 cal CE, but not at 1600 cal CE. Graminoid fractions remained relatively stable, with the exception

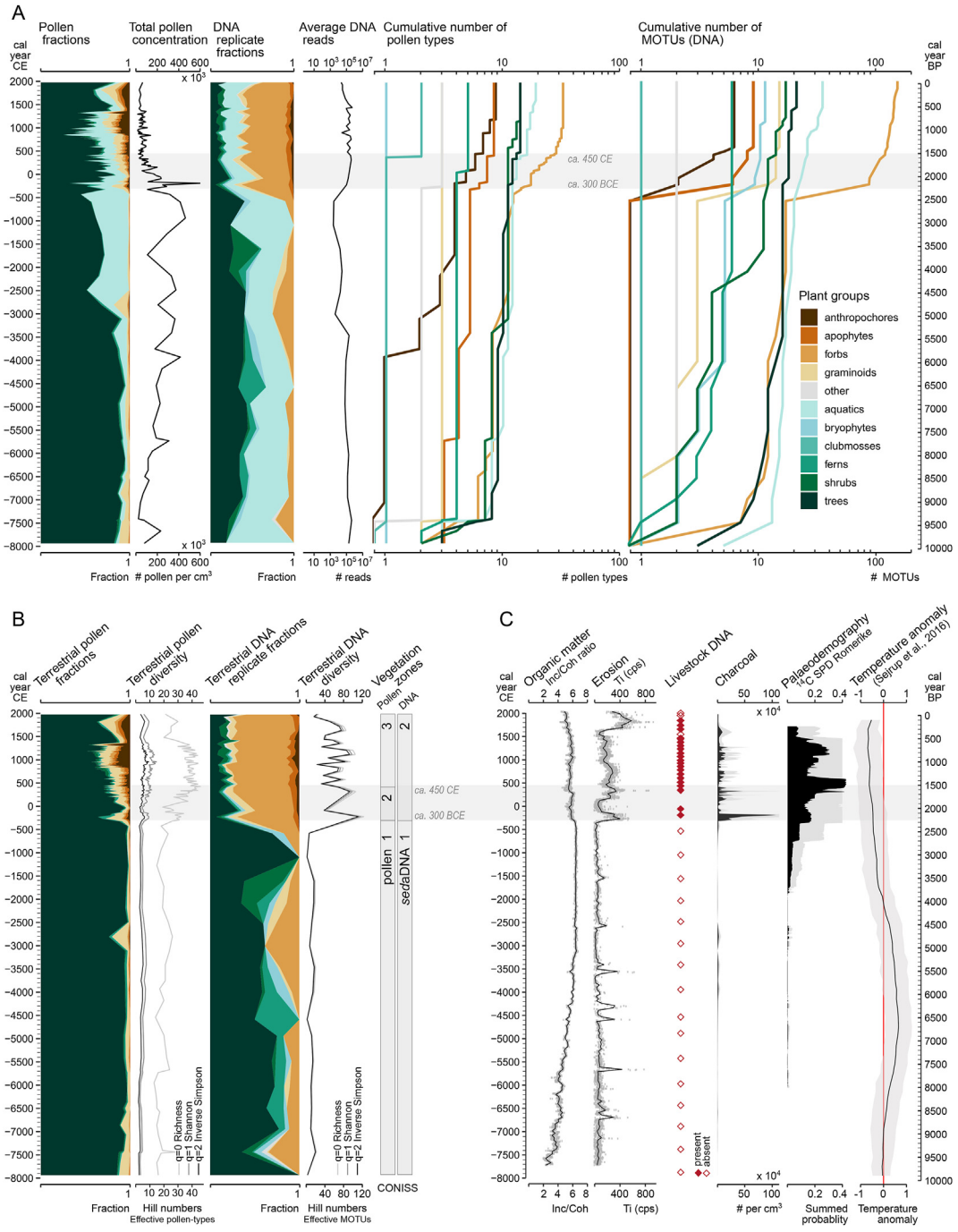

Fig. 3. Overview of the environmental data from Lake Ljøgottjern and the surrounding area. A) the total vegetation fractions of the anthropochores, apophytes, forbs, graminoids, other, aquatics, bryophytes, clubmosses, ferns, shrubs and trees in the pollen and the plant DNA datasets, the total pollen concentration per sample, the summed number of DNA reads per sample, and the cumulative number of taxa in the pollen dataset and the plant DNA dataset for each plant group. Grey shading indicates time periods of considerable cumulative increases in plant taxa. B) The terrestrial pollen fractions, terrestrial DNA replicate fractions and the terrestrial plant diversity determined by Hill numbers, with q = 0, 1, and 2, representing the effective number of taxa (pollen-types or MOTUs) in the form of species richness, Shannon index and inverse Simpson index, respectively. Statistically different vegetation zones were determined through CONISS analysis, identifying ~400 cal BCE and 450 cal CE as boundaries between zones. C) An overview of the environmental variables, including data from the sediment core: organic matter content (Inc/Coh ratio), Ti, presence/absence of livestock DNA, and the charcoal concentration. For the Inc/Coh ratio and Ti, grey points represent all data points and black lines represent smoothed data values derived using a general additive model (GAM). The radiocarbon summed probability densities (^{14}C SPD) are from the Romerike region (Loftsgarden and Solheim, in press) and the median composite temperature anomaly ($\pm 1\sigma$) from 74 lake and marine sites in the North Atlantic-Fennoscandian region as determined by Sejrup et al. (2016).

of two marked decreases in both pollen and *sed*aDNA records at 1000 and 1350 CE.

The increased anthropochore pollen concentrations before ~450 CE were followed by a steady decrease to <2% in the 700–800 cal CE period, which was also apparent in the *sed*aDNA record. Both anthropochore and apophyte fractions in the *sed*aDNA dataset then showed a distinct increase towards ca. 850–1300 cal CE directly followed by decreased fractions. This pattern was matched by anthropochore pollen fractions, with a distinct peak (28%) after 1300 cal CE and a sharp decline (<4%) after 1350 cal CE, while apophyte pollen fractions fluctuated between ca. 2 and 6% throughout this zone.

4.5. Palaeodemographic dynamics

Most radiocarbon dates for the ^{14}C Summed Probability Distributions (SPD) of the Romerike region were dated to the Late Iron Age and the resulting curves largely match the charcoal concentrations in the Lake Ljøgottjern sediment (Fig. 3B; Appendices B.1 and B.6). Charcoal was detected from 7450 cal BCE onwards, throughout most of the sediment core (except for 3 samples) and generally in concentrations below 10×10^4 pieces per cm^3. The ^{14}C SPD record starts at 6050 BCE and trace values (<0.01) were found between 6050 and 4000 cal BCE. Both records showed higher values around 2800 cal BCE, with peaks in charcoal between 4000 and 2800 cal BCE and peaks in ^{14}C SPD values between 2850 and 2650 cal BCE. Values of both proxies remained low in the subsequent period, until 2000 cal BCE when ^{14}C SPD values increased. Charcoal concentrations remained low until 600 cal BCE, when they increased and peaked at 200 cal BCE with a concentration of around 11×10^5 pieces per cm^3. The peak in charcoal matches an increase in ^{14}C SPD for the Romerike region and a distinct short peak is evident in both records at around 300 cal CE (at 270 cal CE for ^{14}C SPD and 320 cal CE for charcoal). More stable high ^{14}C SPD values (>0.35) were recorded between 330 and 550 cal CE when they dropped to <0.2 at 600 cal CE while charcoal concentrations at Lake Ljøgottjern remained relatively stable. Another period of high ^{14}C SPD values (>0.25) was found between ca. 1050 and 1250 cal CE.

4.6. Traces of farming

4.6.1. Cultivated plant taxa

Isolated peaks of *Cannabis/Humulus*-type (hemp and hop), *Hordeum/Avena*-type (barley and oats), *Triticum* (wheat) and *Secale* (rye) pollen concentrations were identified in the period between ca. 4000 and 400 cal BCE. From between 400 and 250 cal BCE a more stable presence of all these pollen types was established. *Linum* (flax) pollen was detected occasionally from 900 cal CE onwards (Fig. 4).

No DNA from cultivated plants was recorded before 230 cal BCE, at 230 cal BCE *Hordeum* (barley) and *Triticum* (wheat) was found in 4 and 2 replicates out of 6 respectively. *Triticum* DNA was not detected in any other samples. The first detection of *Hordeum* DNA matches a peak in *Hordeum/Avena*-type pollen at this time point, which was followed by a decrease in pollen concentration, whereas the *Hordeum* DNA was found in most PCR replicates up until 1350 cal CE. At 300 cal CE *Humulus* DNA and *Linum* DNA were first detected, followed by *Cannabis* at ca. 500 cal CE.

4.6.2. Livestock DNA

DNA from pastoral animals was first detected in the sample dated to 230 cal BCE from cattle, pig and horse (*Bos* sp., *Sus scrofa*, and *Equus* sp.; Fig. 4). From 230 cal BCE onwards, cattle DNA was continuously present, with exceptions at 1500 CE and after 1800 CE when no cattle DNA was detected. Between 230 cal BCE and 450 cal CE, horse DNA was detected in all samples, and sheep DNA (*Ovis* sp.) from 100 cal BCE onwards, while pig DNA was only found at 230 cal BCE. Horse and pig DNA were occasionally present in the 500–1350 cal CE period, whereas sheep DNA was continuously present between 750 and 1420 cal CE. DNA from goat (*Capra* sp.) was detected in two samples: 1110 and 1270 cal CE. At 1520 cal CE, no livestock DNA was found, however, DNA from sheep was present at 1630 cal CE, and both cattle and horse DNA were detected between 1630 and 1820 cal CE.

4.6.3. Archaeological evidence

The earliest settlements were dated to the Bronze Age (ca. 1800–500 BCE; A-ID 96260; Helliksen, 1997) representing one farmstead located north-east of Lake Ljøgottjern (Fig. 1C). A 1994–95 excavation identified seven houses and 105 hearths, with most radiocarbon dates falling within the 1500–200 BCE period (Helliksen, 1997). This farmstead was divided into several farms located closer to the lake during the Iron Age (ca. 550 BCE–1050 CE; A-ID 121551, 171660; Helliksen, 1997; Simonsen, 1997), with the settlement site just north of the medieval farmstead of Haug (A-ID 171660) dated to ca. 800–1050 CE. The farms of Haug (ca. 1390 CE) and Ljøgot (1514 CE) were mentioned in medieval sources (Rygh, 1898, pp. 322–323) and archaeological excavations, finds and historical maps confirm the location of the farmsteads close by the lake, as well as written sources indicating land-use for livestock and crop cultivation (Nesten, 1951).

4.7. Environmental terms related to plant community changes

Distance-based redundancy analysis (dbRDA) of the pollen data reveals that the temperature anomaly explains 5.1% of the variance in terrestrial plant composition ($p = 0.001$), followed by organic matter content (Inc/Coh ratio 4%; $p = 0.001$), presence/absence of livestock (2.4%; $p = 0.003$), Ti (1.8%; $p = 0.017$), and ^{14}C SPD (1.5%; $p = 0.043$; Fig. 5A&B). The same analysis for the *sed*aDNA samples indicates presence/absence of livestock as explanation for 7% of the variance ($p = 0.001$), followed by temperature (6%; $p = 0.006$), organic matter content (5.5%; $p = 0.014$) and Ti (3%; $p = 0.092$; Fig. 5A&B; Appendix A.11). Variation partitioning indicates the highest joint effect of temperature anomaly and presence/absence of livestock on variation in plant community composition for both the pollen samples (31%) and the *sed*aDNA samples (28%). For *sed*aDNA samples, this is followed by the joint effect of presence/absence of livestock and Ti (15%). For pollen samples, the second highest joint effect is of temperature anomaly and ^{14}C SPD (21%; for detailed variation partitioning results see Appendix A.12).

DbRDA of subsections of the core shows that the variance in terrestrial plant assemblages in zone 1 (ca. 8000–300 cal BCE) are related to Ti (20%; $p = 0.001$), organic matter (16%; $p = 0.001$) and temperature (16%, $p = 0.001$) based on the *sed*aDNA data, compared to organic matter (27%; $p = 0.001$) and temperature (9.3%; $p = 0.007$) for the pollen data (Fig. 5B, Appendix A.11). For zone 2 and 3 (ca. 300 cal BCE–1800 cal CE) temperature and ^{14}C SPD are found to best explain the variance in terrestrial plant assemblages based on both the *sed*aDNA (9.7%; $p = 0.008$ and 8.4%; $p = 0.03$) and pollen data (28%; $p = 0.001$ and 3.9%; $p = 0.001$), followed by Ti (3.1%; $p = 0.004$) only for the pollen data.

Temperature anomaly data is highly correlated with sample age ($r_s = 0.93$, $p = 0.000$, $N = 120$) and we found similar relationships for these variables with other environmental terms (Fig. 5C, Appendix A.13). Significant relationships are found between sample age and plant diversity, livestock presence/absence, charcoal, and Ti for both the *sed*aDNA and pollen datasets. Palaeodemographic trends (^{14}C SPD) are significantly correlated with sample age at the time resolution of the pollen data, but not of the *sed*aDNA data. Positive relationships between plant diversity, livestock, charcoal, ^{14}C SPD and Ti are evident for both datasets. Organic matter (Inc/Coh ratio) is not correlated with other environmental terms when considering the entire core, however, in the period from ca. 8000–300 cal BCE they show a significant relation with ^{14}C SPD ($r_s = 0.6$, $p = 0.02$, $N = 120$) and sample age ($r_s = -0.95$, $p = 0.000$, $N = 120$).

5. Discussion

In this study we applied an interdisciplinary approach to uncover anthropogenic and environmental drivers of biological change during the Holocene at Lake Ljøgottjern. Analysis of pollen,

Fig. 4. Anthropochore and apophyte fractions of terrestrial pollen fractions and terrestrial DNA replicate fractions and a selection of plant and mammal taxa associated with humans. Grey shading of pollen concentrations shows 3× exaggerated concentrations while the grey band across individual graphs indicates the time period of pollen zone 2 based on CONISS analysis between ca. 300 BCE and 450 CE.

*sed*aDNA, geochemical and archaeological data enabled us to reconstruct the palaeoenvironmental dynamics and establish a timeline of cultivation and pastoralism at Lake Ljøgottjern for the last 10,000 years while analysing driving factors of biological change. We argue for an integrated approach in the reconstruction of palaeoenvironmental dynamics to better understand past and present human-environment interactions.

5.1. Stratigraphic integrity of the sediment record

We investigated individual and combined analyses of the proxies to infer the stratigraphic integrity of the core for the last 10,000 years. The lithological description and XRF analysis show an abrupt change in the sedimentation rate at ca. 280 cm depth dated to ca. 350 cal BCE (Fig. 2) concurrent with the stratigraphic zonation based on CONISS analysis of pollen and *sed*aDNA, between 430 and 320 cal BCE. Stratigraphic zonation and the separation of NMDS clusters are consistent between pollen and plant *sed*aDNA analysis (Appendices A.9 and A.10), and direct comparison of plant taxa presence between pollen and *sed*aDNA records revealed consistent distributions of plant DNA, strongly indicating that disturbance or leaching do not impact the sedimentary record of Lake Ljøgottjern. This is evident in overall patterns of pollen and plant *sed*aDNA fractions (Fig. 3A and B) as well as specific plant taxa (Fig. 4, Appendices A.7 and A.8), thereby confirming the stratigraphic integrity of the record. Additionally, the pattern in the number of positive replicates for *Cannabis* DNA over time matches the dynamics in the concentrations of *Cannabis/Humulus*-type pollen, with peaks in both records at 950–1200 cal CE and 1350–1450 cal CE, even though pollen is an unlikely source of chloroplast DNA (Parducci et al., 2017; Sjögren et al., 2017). The apparent absence of DNA leaching is consistent with other lake *sed*aDNA records (Alsos et al, 2018, 2020, 2018; Epp et al., 2015). Moreover, plant DNA was detected throughout the sediment core, but mammal DNA was only found in samples dating from 230 cal BCE to 1800 cal CE, indicating that these sequences are unlikely to be a result of contamination. The lithology, geochemistry and the biological data therefore support the stratigraphic integrity of the analysed sequence and the authenticity of the *sed*aDNA.

5.2. Source of pollen and sedaDNA in Lake Ljøgottjern

Both pollen and *sed*aDNA data are affected by source productivity and taphonomic processes of dispersal, transfer, deposition and preservation (Giguet-Covex et al., 2019; Prentice, 1985). Primary sources of animal DNA are urine and faeces and it has been proposed that scattered distributions of animals can result in non-detection of DNA, while enclosures or folds within a lake catchment area can represent a "point source", concentrating the supply of mammal DNA to the lake sediments (Giguet-Covex et al, 2014, 2019). *Sed*aDNA of plants similarly originates from the lake catchment area and is of local provenance (Alsos et al., 2018; Giguet-Covex et al., 2019), whereas pollen may originate from a wide area (Birks and Bjune, 2010). The relevant source area of pollen (RSAP) is dependent on the relative pollen productivity (RPP) of plant taxa and correlated to the size of the lake, with records from small lakes (50 m radius) consisting for 30–45% of pollen originating from within 300–400 m from the lake edge, or 600–800 m for lakes with a 250 m radius (Sugita, 1994). Estimations of RSAP values for small-size lakes (25–250 m radius) in southern Scandinavia fall within ca. 900–2500 m distance from the lake centre, with RSAP values of ca. 1000 m for lakes of 100 m radius in southern Sweden (Sugita et al., 1999), within ca. 1000–2500 m for simulation tests using a 50 m lake radius (Hellman et al., 2009), and ca.

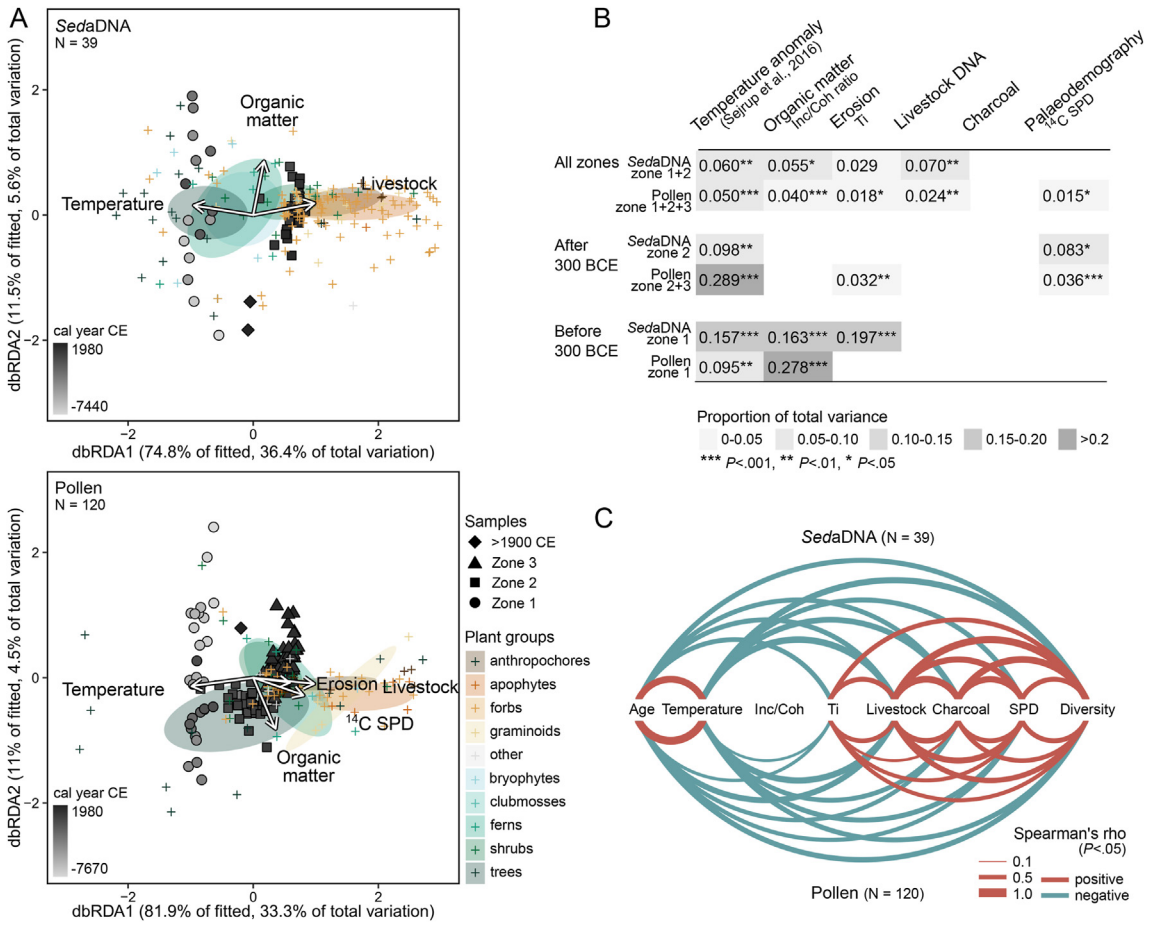

Fig. 5. Summary of automatic stepwise ordinations of plant assemblages using distance-based redundancy analysis (dbRDA). Environmental terms included in dbRDAs: surface temperature anomaly data from Sejrup et al. (2016), organic matter corresponds to the Inc/Coh ratio determined by XRF analysis, Ti is measured by XRF analysis, livestock corresponds to presence/absence of livestock DNA, charcoal corresponds to the charcoal concentrations determined by palynological analysis, and ^{14}C SPD corresponds to radiocarbon summed probability distributions, a proxy for palaeodemography. A) *Sed*aDNA (top) and pollen (bottom) dbRDA ordination sample scores (filled symbols) and plant taxa scores (plus symbols) coloured per plant group. Ellipses indicate the standard error of the mean per plant group. Arrows indicate significant environmental terms. B) Proportions of variance explained per environmental term of the total variance in plant assemblages for six automatic stepwise dbRDAs based on: samples from all zones combined, samples from after 300 BCE, and samples from before 300 BCE for *sed*aDNA and pollen datasets. Blank cells indicate that the environmental term was not included in the model as inclusion did not result in a better model (increased adjusted R2). C) Spearman's rank order correlations for environmental terms included in the dbRDAs of *sed*aDNA (top) and pollen (bottom) data, with addition of the sample age (cal year BP) and diversity (Hill q = 2; inverse Simpson). Line thickness indicates the strength of the correlation in Spearman's rho value and only significant correlations are shown according to Bonferroni adjusted p-values correcting for multiple tests ($p < 0.05$).

900–1100 m for lakes of a 37–247 m (mean: 125 m) radius in western Norway (Hjelle and Sugita, 2012). For Lake Ljøgottjern, with a radius of ca. 60–80 m, this implies a RSAP of at least 900 m. We found many pollen grains from wind-pollinated species (e.g. trees and graminoids), with higher RPPs compared to plants with other forms of reproduction, corroborating that their pollen can come from a much larger distance (Birks and Bjune, 2010; Hjelle and Sugita, 2012; Sugita et al., 1999). On the other hand, *sed*aDNA originates from within the lake catchment, 60 to maximum 230 m distance from the lake edge (Fig. 1C). The vegetation changes inferred from these two proxies therefore reflect environmental dynamics at different scales.

5.3. Palaeoenvironmental history

5.3.1. Ecological succession (ca. 8000–300 cal BCE)

Pollen and *sed*aDNA analyses from the earliest period covered by the core (ca. 8000–4000 cal BCE) revealed low terrestrial plant diversity throughout this period, despite the high rate of plant taxa accumulation found between 8000 and 7000 cal BCE, suggesting a turnover of plant taxa. This turnover is associated with an increase in organic matter content during this period which can reflect an increase in lake productivity or the development of the soils in the lake catchment. The earliest stage of the vegetation record is dominated by *Pinus*, adapted to cold conditions, and *Betula*, a known pioneer. Pollen analysis further revealed the presence of other known pioneer taxa, including *Artemisia*, *Filipendula* and *Rumex* already from the oldest sample (7930 cal BCE). Taxa that are more dependent on fertile soils came into the record at a later time, such as *Urtica* at 5670 cal BCE (Behre, 1981). We also found some *Cannabis/Humulus*-type pollen already at 7000 cal BCE, which are likely from wild *Humulus lupulus* L. as other anthropochore pollen (*Hordeum/Avena*-type, *Triticum* and *Secale*) were not recorded until 3800–1300 cal BCE.

Climate proxy data from Sejrup et al. (2016) showed an increase in temperature between ca. 7000 and 5000 cal BCE, indicating a transition to the Holocene Thermal Maximum, a period ca. 5000–2200 cal BCE characterised by warm and dry summers in the Northern Hemisphere (Antonsson and Seppä, 2007; Wanner et al., 2011). We accordingly found increased concentrations of thermophilic trees, including *Ulmus*, *Corylus*, *Alnus*, and from ca. 4500 cal BCE also *Quercus* and *Tilia*. Ti remained low, with peaks indicating a

number of erosion events during the Holocene Thermal Maximum. Similar frequent flood events during the warm early and middle Holocene in southern Norway have been identified as intense summer rainstorms based on the sedimentary composition (Støren et al., 2016). Erosion rates can affect the representation of the catchment vegetation in the *sed*aDNA record (Giguet-Covex et al., 2019). Indeed, Ti variations in zone 1 of the sediment core (ca. 8000–300 cal BCE) were found to be significantly related to the variations in plant communities as recovered by *sed*aDNA analysis, but not by pollen analysis. In conclusion, we recognize that the increase in temperature, but also the accumulation of organic matter, are related to the variation in plant communities from pollen and *sed*aDNA analysis and are likely driving factors in ecological succession during this period up to 300 cal BCE at Lake Ljøgottjern.

5.3.2. Early human land-use? (ca. 4000–300 cal BCE)

Many vegetation reconstructions from southeastern Norway (such as from Rud Øde, Danielsetermyr, and Skogstjern; Fig. 1A and B) shows an overall progression from the possible presence of hunter-gatherers recorded in the charcoal records, through the establishment of pastoral farming to either mixed farming or cereal cultivation (Høeg, 1996, 1996, 1996; Wieckowska-Lüth et al., 2017), as is the case for Lake Ljøgottjern (this study). The exact timing of these transitions differs between localities. Pastoralism can be inferred indirectly through presence of plant taxa that are favoured by the presence of livestock, through animal faeces, trampling and selection through consumption. Such taxa include nitrophilous and ruderal species, e.g. *Rumex* sp., *Urtica* sp., *Chenopodium* sp. and *Plantago* sp. (Behre, 1981). Over half of the locations indicated in Fig. 1 show the first indications of pastoral farming concurrent with the Early Neolithic (ca. 4000–3300 BCE; Skogstjern, Sveskestutjern, Danielsetermyr, Bånntjern in Tolga, and Ljøgottjern) and Middle Neolithic (ca. 3300–2400 BCE; Rud Øde, Bånntjern in Ullensaker, Skånetjern, Stortallsjøen, Lensmannsvollen, Kåsmyra, Hellemundsmyra, Skjerdingsfjell, and Hirsjøen), while other locations record the first signs of pastoralism anytime between ca. 2000 BCE and 1800 CE (Høeg, 1997; Høeg, 1996; Wieckowska-Lüth et al., 2017, Fig. 1A and B). In this study, we found peaks in concentrations of several of these taxa reflected in increased apophyte fractions in the periods of ca. 5500 cal BCE, 4000–1700 cal BCE, and 950–500 cal BCE (Fig. 4), matching other pollen records from the Romerike region that showed some indications for grazing already in the Early Neolithic (4000–3300 BCE; Danielsetermyr and Svenskestutjern) and Middle Neolithic (3300–2400 BCE; Rud Øde, Bånntjern in Ullensaker, and Skånetjern). The absence of *sed*aDNA of pastoral animals at Lake Ljøgottjern during this time could be due to scattered distribution or pastoral activities taking place outside of the lake catchment area (Giguet-Covex et al., 2019).

Early detection of anthropochore pollen (e.g. *Cannabis/Humulus*-type, *Hordeum/Avena*-type and *Secale*) between ca. 3800 and 2500 cal BCE at Lake Ljøgottjern matches peaks in charcoal. The new high resolution pollen record further showed an increase in concentrations of graminoids between 4000 and 2500 cal BCE and the *sed*aDNA record indicated a higher diversity in forbs as well as more positive replicates for *Carex* (sedge, a graminoid), both indicating a more open landscape around the lake during this time. The temperature anomaly composite from Sejrup et al. (2016) suggested a still relatively high but decreasing temperature anomaly between 4000 and 2000 cal BCE, which was followed by decreased concentrations in thermophilic trees (*Ulmus*, *Corylus, Alnus, Quercus* and *Tilia*) marking the end of the Holocene Thermal Maximum. These findings are largely concurrent with the earliest indications of cereal cultivation in southeastern Norway in the Middle and Late Neolithic (ca. 3300–1750 BCE; Danielsetermyr, Bånntjern in Ullensaker, Skånetjern, Dulpmoen, Engelaug, Kjerdingsfjell, and Hirsjøen; Høeg, 1996, 1997, Fig. 1A and B), although at Lake Skogstjern the occurrence of *Plantago lanceolata*-type and cereal pollen are both dated to ca. 3650–3400 cal BCE (Wieckowska-Lüth et al., 2017). With the exception of Danielsetermyr, pollen records from the Romerike region and further north indicate a delayed introduction of pastoralism (ca. 3000 BCE) and cultivation (ca. 2500–2000 BCE). Within the Romerike region, the northeastern sites do not attest cereal cultivation before ca. 200 BCE (Høeg, 1997).

For most of the discussed pollen records in southeastern Norway, indicators of pastoralism and cultivation were not continuous from the first detection (Høeg, 1996, 1997) and intensification of farming activities is mostly evident from the Early Iron Age (from 500 BCE–550 CE), consistent with the general intensification of agriculture in southeastern Norway (Mjærum, 2020; Myhre, 2002; Solberg, 2000). Also at Lake Ljøgottjern, we found little evidence for human presence between ca. 2500 and 2000 cal BCE as ^{14}C SPD and concentrations of charcoal and anthropochore pollen returned to values close to zero. ^{14}C SPD values increased again after 2000 cal BCE, followed by indications of cereal cultivation with for example *Triticum* pollen at 1700 cal BCE and *Hordeum/Avena* and *Secale* pollen at 1300 cal BCE, and increased charcoal concentrations from 600 cal BCE coinciding with detection of *Cannabis/Humulus* pollen. These patterns, visible in the pollen record but not in the *sed*aDNA, are in accordance with the archaeological evidence of a Bronze Age settlement at approximately 500 m north-east from the lake, dated to ca. 1800–500 BCE (A-ID96260; Fig. 1C).

5.3.3. Intensification of agriculture and pastoralism (ca. 300 cal BCE–present)

From ca. 300 cal BCE taxonomic diversity at Lake Ljøgottjern increased rapidly (Fig. 3A and B), most notable in the *sed*aDNA record in which crops and livestock appeared for the first time at 230 cal BCE. From this time onwards, also plant taxa associated with pastoral farming (*Rumex* sp., *Urtica* sp., *Chenopodium* sp. and *Plantago* sp.; Behre, 1981) were consistently present in both *sed*aDNA and pollen records. Moreover, increases in Ti and charcoal concentrations were observed (Fig. 3C), suggesting more erosion through anthropogenic activities such as pastoralism and the development of an agricultural landscape (Giguet-Covex et al, 2014, 2019). The simultaneous decrease in organic matter despite pastoral activities during this period is likely caused by the increased erosion. Overall, all these proxies indicate intensified human activity, consistent with pollen records from the Romerike region that indicate widespread grazing activity in the region from the Early Iron Age (Figs. 3 and 500 BCE–550 CE; Høeg, 1997) and the general intensification of agriculture in southeastern Norway (Mjærum, 2020; Myhre, 2002; Solberg, 2000). At Lake Ljøgotjern we can trace, from the *sed*aDNA and Ti records, the abrupt changes in the local environment resulting from the establishment of one or multiple farms in close proximity to the lake, as evident by several archaeological sites and finds (A-ID 121551, 171659, 171592, 173761, 172010 and 180,779; Fig. 1C).

During the past 2000 years we can recognize periods of decreased versus intensified human activity. During ca. 150 cal BCE to 100 cal CE reduced pollen diversity, lower numbers of detected anthropochore taxa, decreased charcoal concentrations and ^{14}C SPD values as well as lower Ti suggest a reduction in the nearby human population or at least in their activities in the local surroundings. A subsequent peak in charcoal concentrations and ^{14}C SPD at 300 cal CE matches the first detection of *Humulus* and *Linum* in the *sed*aDNA record. Between ca. 300 and 600 cal CE we found relatively high concentrations of apophyte pollen, coinciding with detection of cattle, horse and sheep DNA, indicating pastoral activities. A change in the pollen record at 450 cal CE (detected by the

CONISS analyses) is driven by the first detection of *Spergularia* pollen and increased concentrations of anthropochore pollen, coinciding with the first finding of *Cannabis* DNA, suggesting the intensification of agricultural practices. Also ^{14}C SPD values were high between 330 and 550 cal CE, while temperature anomalies were relatively low (Sejrup et al., 2016). A second period of relatively high ^{14}C SPD values was identified ca. 1050–1250 cal CE, corresponding with a continued presence of livestock DNA (from cattle, pigs, sheep and goats), anthropochore DNA (*Linum*, *Hordeum* and *Cannabis*), and high concentrations of anthropochore pollen during the Medieval warm period (ca. 800–1300 CE). A settlement site just north of the medieval farmstead of Haug is dated to this period (ca. 800–1050 CE; A-ID 171660; Helliksen, 1997, Fig. 1C) and may be related to this increase. Medieval sources mention the farms of Haug (ca. 1390 CE) and Ljøgot (1514 CE) with locations of their farmsteads close to the lake (Rygh, 1898, pp. 322–323; Fig. 1C). *Sed*aDNA, pollen and written records (Nesten, 1951) all indicate mixed farming activities with cattle, sheep and cultivation of cereals, oats, hemp and flax during this time. At 1520 cal CE, however, no livestock DNA was detected and anthropochore DNA reduced to oats and flax (Fig. 4). Anthropochore pollen fractions peaked again around 1700–1800 cal CE, matching the returned presence of livestock between 1630 and 1820 cal CE while little evidence of anthropochores was present in the *sed*aDNA record at this time, suggesting a focus on pastoral farming within the lake catchment area of specifically cattle and horse. Modern samples (>1800 cal CE) showed limited plant diversity, no presence of livestock and indicate a focus on the cultivation of *Hordeum* in close vicinity of the lake reflected by its presence in the *sed*aDNA record, while *Triticum* was only found in the pollen record and therefore likely cultivated outside of the lake catchment area. These results reflect modern (mono) cultivation with no or reduced alternation in land use, and animals possibly receiving water from established small ponds as identified on historical maps.

Between 300 cal BCE and 1800 cal CE temperature explained most of the variation in plant composition followed by palaeodemography (Fig. 5B). During this period, ^{14}C SPD values increased and peaked earlier at ca. 330–550 cal CE and 1050–1250 cal CE, matching high detection of DNA from pastoral animals and increased apophyte and anthropochore concentrations. Temperature anomaly decreased in Scandinavia and was especially low around ca. 450 CE and 1250–1650 CE (Sejrup et al., 2016), with the first cold period matching the change in the pollen record marking the subsequent intensification of agricultural activities, while the 1250–1650 CE cold period showed decreasing trends in anthropochore pollen and *sed*aDNA fractions, suggesting decreased agricultural activities during colder periods. In summary, we found that the variation in surface temperature anomaly and ^{14}C SPD relate to the variation in plant communities from pollen and *sed*aDNA analysis and observed several periods of intensified mixed farming activities, likely driven by increasing human population densities.

5.4. The role of anthropogenic and environmental factors

Previous studies have emphasized the long-term role of humans in shaping our modern ecosystems through their use of land (Boivin and Crowther, 2021; Ellis, 2015; Stephens et al., 2019; Williams et al., 2015), with the timing of human land-use transitions likely reflecting cultural, ecological and climatic shifts (Boivin et al., 2016). In this study, estimates of human population density, pastoralism, surface temperature, erosion and organic matter all correlated significantly with changes in plant communities during the Holocene, especially at ca. 300 cal BCE (Fig. 5A&B). However, the importance of each of these factors changed over time and most of the included environmental terms correlated with sample age (Fig. 5C). Moreover, analyses of subsections of the data from specific time periods (i.e. pollen and *sed*aDNA zones; Fig. 3) affected results (Fig. 5B), indicating the importance of an analytical basis for the choice of time period to include in these types of analyses.

Climate played an important role in early postglacial succession of plants, together with soil maturation, competition for light and plant migration patterns (Antonsson and Seppä, 2007). Surface temperature is a climatic parameter for which reliable long-term proxies exist and is related not only to vegetation change, but also to human land-use (Warden et al., 2017). Indeed, surface temperature and the accumulation of organic matter were strongly related to the variation in plant communities at Lake Ljøgottjern from ca. 8000 to 300 cal BCE. Significant relationships between surface temperature anomaly and the change in plant community were found in the separate vegetation zones as well as throughout the entire studied period of the last 9000 years (Fig. 5A&B). The strong role of temperature in the vegetation dynamics, also illustrated by increased pollen concentrations of thermophilic tree taxa during the Holocene Thermal Maximum, is in agreement with the general ecological understanding that temperature is one of the main limiting factors for the northern limits of temperate tree taxa (Jackson et al., 2009; Woodward et al., 2004). Other studies quantifying the role of anthropogenic and environmental factors similarly indicate climate as the major driver of vegetation composition throughout the Holocene and especially before the introduction of agriculture (Kuosmanen et al., 2018; Marquer et al., 2017; Reitalu et al., 2013). We further identified significant negative relationships between temperature and all of the environmental changes associated with human presence, i.e. ^{14}C SPD, charcoal, diversity, and increased erosion (Fig. 5C). No clear statistical relationships between these environmental changes were found within the separate time periods (8000–300 cal BCE and 300 cal BCE–1800 cal CE; Appendix A.12).

In the more recent period, ca. 300 cal BCE–1800 cal CE, variations in plant communities at Lake Ljøgottjern were related to surface temperature, ^{14}C SPD, and Ti, with evidence of more intense farming during periods of high population density based on the intensification of anthropochore pollen, which were followed by periods of lower temperatures. Some variation in the presence of pastoral animals was observed, but as we focused on the presence and absence of livestock as a conservative estimate of pastoral activities at Lake Ljøgottjern, inferences about the intensity of pastoral activities are limited. Nevertheless, plant community composition and presence/absence of livestock were significantly related when including all zones in the stepwise dbRDA (Fig. 5B). However, this relationship was not evident within individual zones. Similarly, many correlations between pairs of environmental terms, particularly relating to human activities (charcoal, ^{14}C SPD, livestock and Ti), were only found when including both 8000–300 cal BCE and 300 cal BCE–1800 cal CE time periods, strongly suggesting that the transition between the two vegetation zones was primarily a result of anthropogenic impacts. The onset of strong human impacts on vegetation through the intensification of agriculture in the wider area of southeastern Norway has been dated to the Early Iron Age (500 BCE–550 CE; Høeg, 1997; Mjærum, 2020; Myhre, 2002). Similar increased roles of anthropogenic factors on plant communities during the late Holocene have been previously found for Sweden and Finland (Kuosmanen et al., 2018) associated with growing human population size, and for Estonia (Reitalu et al., 2013) and Europe (including Scandinavia and the Baltic; Marquer et al., 2017) associated with the establishment and expansion of agriculture.

6. Conclusions

Past human land-use has had a major impact on our ecosystems

and knowledge about the role of cultural, ecological and climatic factors in driving these changes is important for understanding how our modern ecosystems were shaped. Distinguishing anthropogenic and environmental drivers of biological change requires integrated analyses of long-term records from a diversity of disciplines, combining knowledge about the local human history as well as climatic and other environmental changes. Using evidence from high-resolution pollen, *sed*aDNA and geochemical analysis from the same lake sediment core, combined with archaeological evidence of local human settlement and regional population dynamics we were able to obtain a detailed reconstruction of complex anthropogenic and environmental dynamics affecting the vegetation at Lake Ljøgottjern for the last 10,000 years of the Holocene.

Although the exact timing of transitions to pastoralism and cereal cultivation differ between localities, the timing of these transitions at Lake Ljøgottjern are concurrent with multiple other locations in southeastern Norway. Pollen and *sed*aDNA analyses reflected vegetation at different spatial scales matching the archaeological evidence of the establishment of Bronze Age (ca. 1800–500 BCE) and Iron Age (ca. 550 BCE–1050 CE) farms at varying distances from the lake. Together, they provide a detailed timeline of cultivation and pastoralism. Our statistical analyses demonstrate that vegetation changes were primarily related to natural processes during most of the Holocene (ca. 8000–300 cal BCE), up until the Early Iron Age (ca. 500 BCE–550 CE), when human population densities in the region started increasing. Periods of decreased versus intensified human activity could be distinguished in the 300 cal BCE–1800 cal CE time period, with evidence of more intense farming during periods of high population density and possibly related to surface temperatures. This led to a rapid shift in plant communities, presence of livestock, increased erosion and high charcoal concentrations. Together, the integrated multiproxy results from our study show the complex relations between environmental changes, facilitate the understanding of the coupled dynamics of climate, soils, human activities, and vegetation during the Holocene, and specifically highlight the importance of anthropogenic activities in long-term shaping of plant communities.

Author contributions

Conceptualisation ATS, MB, KK, SB, KL, FI; coring JB, ES, MB, EB; core subsampling MB, EB, SB, ATS; geochemical analysis MB, EB; *sed*aDNA and bioinformatic analysis ATS; pollen analysis HH; age-depth modelling MB; summed probability distribution analysis KL; archaeological analysis FI; validation of *sed*aDNA identifications AK, AB; statistical analysis and writing original draft ATS; review and editing SB, KK, MB, KL, FI. All co-authors commented on the manuscript.

Data availability

All raw read data are available at the European Nucleotide Archive (ENA) under study accession number PRJEB44988. Scripts for read data processing are available at https://github.com/terschure/dataprocessing_LJO. All processed data are available in the supporting information of this article.

Declaration of competing interest

The authors declare that they have no known competing financial interests or personal relationships that could have appeared to influence the work reported in this paper.

Acknowledgements

This work contributes to the FRIPRO Toppforsk project VIKINGS "Volcanic Eruptions and their Impacts on Climate, Environment, and Viking Society in 500–1250 CE", funded by the Research Council of Norway (project number 275191). The two coring campaigns and the XRF geochemistry were conducted within the National infrastructure EARTHLAB (NRC 226171) at the University of Bergen. This work was supported by the Research Council of Norway Centres of Excellence CEED project 223272. Financial support was provided by the Faculty of Mathematical and Natural Sciences, University of Oslo. We thank the Norwegian Sequencing centre for their advice and DNA sequencing. DNA analyses were performed on the Saga computer cluster, owned by the University of Oslo and Uninett/Sigma2, and operated by the Department of Research Computing at USIT, University of Oslo.

Appendix A. Supplementary data

Supplementary data to this article can be found online at https://doi.org/10.1016/j.quascirev.2021.107175.

References

Alsos, I.G., Sjögren, P., Edwards, M.E., Landvik, J.Y., Gielly, L., Forwick, M., et al., 2016. Sedimentary ancient DNA from Lake Skartjørna, Svalbard: assessing the resilience of arctic flora to Holocene climate change. Holocene 26 (4), 627–642.

Alsos, I.G., Lammers, Y., Yoccoz, N.G., Jørgensen, T., Sjögren, P., Gielly, L., Edwards, M.E., 2018. Plant DNA metabarcoding of lake sediments: how does it represent the contemporary vegetation. PloS One 13 (4), e0195403.

Alsos, I.G., Sjögren, P., Brown, A.G., Gielly, L., Merkel, M.K.F., Paus, A., et al., 2020. Last Glacial Maximum environmental conditions at Andøya, northern Norway; evidence for a northern ice-edge ecological "hotspot". Quat. Sci. Rev. 239, 106364.

Antonsson, K., Seppä, H., 2007. Holocene temperatures in Bohuslän, southwest Sweden: a quantitative reconstruction from fossil pollen data. Boreas 36 (4), 400–410.

Arnaud, F., Poulenard, J., Giguet-Covex, C., Wilhelm, B., Révillon, S., Jenny, J.P., et al., 2016. Erosion under climate and human pressures: an alpine lake sediment perspective. Quat. Sci. Rev. 152, 1–18.

Bajard, M., Bakke, J., Støren, E., Ballo, E., Høeg, H., Iversen, F., Loftsgarden, K., Svensen, H. & Krüger, K. (Submitted). Climate variability controlled the pre-Viking society development during the Late Antiquity in Eastern Norway.

Bajard, M., Poulenard, J., Sabatier, P., Bertrand, Y., Crouzet, C., Ficetola, G.F, et al., 2020. Pastoralism increased vulnerability of a subalpine catchment to flood hazard through changing soil properties. Palaeogeogr. Palaeoclimatol. Palaeoecol. 538, 109462. https://doi.org/10.1016/j.palaeo.2019.109462.

Bajard, M., Poulenard, J., Sabatier, P., Etienne, D., Ficetola, F., Chen, W, et al., 2017. Long-term changes in alpine pedogenetic processes: effect of millennial agro-pastoralism activities (French-Italian Alps). Geoderma 306, 217–236. https://doi.org/10.1016/j.geoderma.2017.07.005.

Bajard, M., Sabatier, P., David, F., Develle, A.L., Reyss, J.L., Fanget, B., et al., 2016. Erosion record in lake La thuile sediments (Prealps, France): evidence of montane landscape dynamics throughout the Holocene. Holocene 26 (3), 350–364.

Behre, K.E., 1981. The interpretation of anthropogenic indicators in pollen diagrams. Pollen et Spores 23, 225–245.

Birks, H.H., Bjune, A.E., 2010. Can we detect a west Norwegian tree line from modern samples of plant remains and pollen? Results from the DOORMAT project. Veg. Hist. Archaeobotany 19 (4), 325–340.

Blaauw, M., Christen, J.A., 2011. Flexible paleoclimate age-depth models using an autoregressive gamma process. Bayesian analysis 6 (3), 457–474.

Boessenkool, S., Epp, L.S., Haile, J., Bellemain, E.V.A., Edwards, M., Coissac, E., et al., 2012. Blocking human contaminant DNA during PCR allows amplification of rare mammal species from sedimentary ancient DNA. Mol. Ecol. 21 (8), 1806–1815. https://doi.org/10.1111/j.1365-294X.2011.05306.x.

Boivin, N., Crowther, A., 2021. Mobilizing the past to shape a better Anthropocene. Nat. Ecol. Evol. 5 (3), 273–284. https://doi.org/10.1038/s41559-020-01361-4.

Boivin, N.L., Zeder, M.A., Fuller, D.Q., Crowther, A., Larson, G., Erlandson, J.M., et al., 2016. Ecological consequences of human niche construction: examining long-term anthropogenic shaping of global species distributions. Proc. Natl. Acad. Sci. Unit. States Am. 113 (23), 6388–6396. https://doi.org/10.1073/pnas.1525200113.

Bonsall, C., Macklin, M.G., Anderson, D.E., Payton, R.W., 2002. Climate change and the adoption of agriculture in north-west Europe. Eur. J. Archaeol. 5 (1), 9–23.

Boyer, F., Mercier, C., Bonin, A., Le Bras, Y., Taberlet, P., Coissac, E., 2016. obitools: a unix-inspired software package for DNA metabarcoding. Mol. Ecol. Res. 16 (1), 176–182.

Chao, A., Gotelli, N.J., Hsieh, T.C., Sander, E.L., Ma, K.H., Colwell, R.K., Ellison, A.M., 2014. Rarefaction and extrapolation with Hill numbers: a framework for sampling and estimation in species diversity studies. Ecol. Monogr. 84 (1), 45–67.
Crema, E.R., Bevan, A., 2021. Inference from large sets of radiocarbon dates: software and methods. Radiocarbon 63 (1), 23–39.
Ellis, E.C., 2015. Ecology in an anthropogenic biosphere. Ecol. Monogr. 85 (3), 287–331. https://doi.org/10.1890/14-2274.1.
Epp, L.S., Gussarova, G., Boessenkool, S., Olsen, J., Haile, J., Schrøder-Nielsen, A., Brochmann, C., 2015. Lake sediment multi-taxon DNA from North Greenland records early post-glacial appearance of vascular plants and accurately tracks environmental changes. Quat. Sci. Rev. 117, 152–163.
Epp, L.S., Zimmermann, H.H., Stoof-Leichsenring, K.R., 2019. Sampling and extraction of ancient DNA from sediments. Methods Mol. Biol. 1963, 31–44.
Faegri, K., Kaland, P.E., Krzywinski, K., 1989. Textbook of Pollen Analysis, fourth ed. John Wiley & Sons Ltd.
Ficetola, G.F., Coissac, E., Zundel, S., Riaz, T., Shehzad, W., Bessière, J., et al., 2010. An *in silico* approach for the evaluation of DNA barcodes. BMC Genom. 11 (1), 1–10. https://doi.org/10.1186/1471-2164-11-434.
Freeman, J., Byers, D.A., Robinson, E., Kelly, R.L., 2018. Culture process and the interpretation of radiocarbon data. Radiocarbon 60 (2), 453–467.
Giguet-Covex, C., Pansu, J., Arnaud, F., Rey, P.J., Griggo, C., Gielly, L., et al., 2014. Long livestock farming history and human landscape shaping revealed by lake sediment DNA. Nat. Commun. 5 (1), 1–7. https://doi.org/10.1038/ncomms4211.
Giguet-Covex, C., Ficetola, G.F., Walsh, K., Poulenard, J., Bajard, M., Fouinat, L., et al., 2019. New insights on lake sediment DNA from the catchment: importance of taphonomic and analytical issues on the record quality. Sci. Rep. 9 (1), 1–21. https://doi.org/10.1038/s41598-019-50339-1.
Grimm, E.C., 1987. CONISS: a FORTRAN 77 program for stratigraphically constrained cluster analysis by the method of incremental sum of squares. Comput. Geosci. 13 (1), 13–35.
Hagen, A., 1997. Gåten Om Kong Raknes Grav: Hovedtrekk I Norsk Arkeologi. Cappelen.
Helliksen, W., 1997. *Gård og utmark på romerrike 1100 f. Kr.-1400 e. Kr: Gardermoprosjektet*. Universitetets Oldsaksamling.
Hjelle, K.L., Sugita, S., 2012. Estimating pollen productivity and relevant source area of pollen using lake sediments in Norway: how does lake size variation affect the estimates? Holocene 22 (3), 313–324.
Hjelle, K.L., Halvorsen, L.S., Prøsch-Danielsen, L., Sugita, S., Paus, A., Kaland, P.E., Midtbø, I., 2018. Long-term changes in regional vegetation cover along the west coast of southern Norway: the importance of human impact. J. Veg. Sci. 29 (3), 404–415. https://doi.org/10.1111/jvs.12626.
Hellman, S., Bunting, M.J., Gaillard, M.J., 2009. Relevant source area of pollen in patchy cultural landscapes and signals of anthropogenic landscape disturbance in the pollen record: a simulation approach. Rev. Palaeobot. Palynol. 153 (3–4), 245–258.
Høeg, H.I., 1996. Pollenanalytiske Undersøkelser I" Østerdalsområdet" Med Hovedvekt På Rødsmoen, Åmot I Hedmark. Universitetets oldsaksamling.
Høeg, H.I., 1997. Pollenanalytiske Undersøkelser På Øvre Romerike: Ullensaker Og Nannestad, Akershus Fylke: Gardermoprosjektet. Universitetets oldsaksamling.
Jackson, S.T., Betancourt, J.L., Booth, R.K., Gray, S.T., 2009. Ecology and the ratchet of events: climate variability, niche dimensions, and species distributions. Proc. Natl. Acad. Sci. Unit. States Am. 106 (Suppl. 2), 19685–19692.
Johnsen, G., 1941. Slekten Koren. Bokstuas forlag, Oslo.
Juggins, S., 2020. *Rioja: Analysis of Quaternary Science Data*. R Package Version 0, pp. 9–26. https://cran.r-project.org/package=rioja.
Kaufman, D., McKay, N., Routson, C., Erb, M., Dätwyler, C., Sommer, P.S., Davis, B., 2020. Holocene global mean surface temperature, a multi-method reconstruction approach. Sci. Data 7 (1), 1–13. https://doi.org/10.1038/s41597-020-0530-7.
Kotov, S., Paelike, H., 2018, December. QAnalySeries-A Cross-Platform Time Series Tuning and Analysis Tool, vol. 2018. AGU Fall Meeting Abstracts. PP53D–1230.
Kuosmanen, N., Marquer, L., Tallavaara, M., Molinari, C., Zhang, Y., Alenius, T., Seppä, H., 2018. The role of climate, forest fires and human population size in Holocene vegetation dynamics in Fennoscandia. J. Veg. Sci. 29 (3), 382–392.
Krause-Kyora, B., Makarewicz, C., Evin, A., Flink, L.G., Dobney, K., Larson, G., Nebel, A., 2013. Use of domesticated pigs by Mesolithic hunter-gatherers in northwestern Europe. Nat. Commun. 4 (1), 1–7. https://doi.org/10.1038/ncomms3348.
Legendre, P., Anderson, M.J., 1999. Distance-based redundancy analysis: testing multispecies responses in multifactorial ecological experiments. Ecol. Monogr. 69 (1), 1–24.
Li, D., 2018. hillR: taxonomic, functional, and phylogenetic diversity and similarity through Hill Numbers. J. Open Source Software 3 (31), 1041.
Loftsgarden, K., Solheim, S., 2021. Uncovering Population Dynamics in Southeast Norway from 1300 BC to 1500 AD Using Summed Radiocarbon Probability Distributions (in press).
Longva, O., Thoresen, M.K., 1989. The age of the Hauerseter delta. Nor. Geol. Tidsskr. 69, 131–134.
Malmström, H., Gilbert, M.T.P., Thomas, M.G., Brandström, M., Storå, J., Molnar, P., Willerslev, E., 2009. Ancient DNA reveals lack of continuity between neolithic hunter-gatherers and contemporary Scandinavians. Curr. Biol. 19 (20), 1758–1762. https://doi.org/10.1016/j.cub.2009.09.017.
Marquer, L., Gaillard, M.J., Sugita, S., Poska, A., Trondman, A.K., Mazier, F., Seppä, H., 2017. Quantifying the effects of land use and climate on Holocene vegetation in Europe. Quat. Sci. Rev. 171, 20–37.
Mjærum, A., 2020. The emergence of mixed farming in eastern Norway. Agric. Hist. Rev. 68 (1), 1–21.
Myhre, B., 2002. Landbruk, landskap og samfunn 4000 f. Kr.–800 e. Kr. *Norges landbrukshistorie I, 400f. Kr.-135 e. Kr. Jorda blir levevei*. Det Norske Samlaget, Oslo, pp. 11–213.
Nelson, G.C., Bennett, E., Berhe, A.A., Cassman, K., DeFries, R., Dietz, T., Zurek, M., 2006. Anthropogenic drivers of ecosystem change: an overview. Ecol. Soc. 11 (2).
Nesje, A., 1992. A piston corer for lacustrine and marine sediments. Arct. Alp. Res. 24 (3), 257–259.
Nesten, H.J.L., 1951. Ullensaker: en bygdebok, vol. 3. Grøndahl & Søns Boktrykkeri.
Oksanen, J., Blanchet, F.G., Friendly, M., Kindt, R., Legendre, P., McGlinn, D., Minchin, P.R., O'Hara, R.B., Simpson, G.L., Solymos, P., Stevens, M.H.H., Szoecs, E., Wagner, H., 2020. Vegan: Community Ecology Package. R Package, pp. 5–7 version 2. https://CRAN.R-project.org/package=vegan.
Pansu, J., Giguet-Covex, C., Ficetola, G.F., Gielly, L., Boyer, F., Zinger, L., Choler, P., 2015. Reconstructing long-term human impacts on plant communities: an ecological approach based on lake sediment DNA. Mol. Ecol. 24 (7), 1485–1498. https://doi.org/10.1111/mec.13136.
Parducci, L., Bennett, K.D., Ficetola, G.F., Alsos, I.G., Suyama, Y., Wood, J.R., Pedersen, M.W., 2017. Ancient plant DNA in lake sediments. New Phytol. 214 (3), 924–942. https://doi.org/10.1111/nph.14470.
Prentice, I.C., 1985. Pollen representation, source area, and basin size: toward a unified theory of pollen analysis. Quat. Res. 23 (1), 76–86.
Price, T.D., 2000. The Introduction of Farming in Northern Europe. Europe's first farmers, pp. 260–300.
R Core Team, 2020. R: A Language and Environment for Statistical Computing (Manual). Vienna, Austria.
Ramette, A., 2007. Multivariate analyses in microbial ecology. FEMS Microbiol. Ecol. 62 (2), 142–160.
Reimer, P.J., Austin, W.E., Bard, E., Bayliss, A., Blackwell, P.G., Ramsey, C.B., Talamo, S., 2020. The IntCal20 Northern Hemisphere radiocarbon age calibration curve (0–55 cal kBP). Radiocarbon 62 (4), 725–757.
Reitalu, T., Seppä, H., Sugita, S., Kangur, M., Koff, T., Avel, E., Veski, S., 2013. Long-term drivers of forest composition in a boreonemoral region: the relative importance of climate and human impact. J. Biogeogr. 40 (8), 1524–1534.
Rick, J.W., 1987. Dates as data: an examination of the Peruvian preceramic radiocarbon record. Am. Antiq. 52 (1), 55–73.
Robinson, D.E., 2003. Neolithic and Bronze Age agriculture in southern Scandinavia—recent archaeobotanical evidence from Denmark. Environ. Archaeol. 8 (2), 145–165. https://doi.org/10.1179/env.2003.8.2.145.
Ruddiman, W.F., 2003. The anthropogenic greenhouse era began thousands of years ago. Climatic Change 61 (3), 261–293.
Ruddiman, W.F., Ellis, E.C., Kaplan, J.O., Fuller, D.Q., 2015. Defining the epoch we live in. Science 348 (6230), 38–39. https://doi.org/10.1126/science.aaa7297.
Rygh, O., 1898. Norske Gaardnavne: Akershus Amt, vol. 2. WC Fabritius, 1898.
Sejrup, H.P., Seppä, H., McKay, N.P., Kaufman, D.S., Geirsdóttir, Á., de Vernal, A., Andrews, J.T., 2016. North Atlantic-Fennoscandian Holocene climate trends and mechanisms. Quat. Sci. Rev. 147, 365–378.
Simonsen, M.F., 1997. Boplasspor. Ljøgot, 137/1, Ullensaker Kommune, Akershus. Rapport Arkeologisk Utgravning.
Simpson, G.L., 2018. Modelling palaeoecological time series using generalised additive models. Frontiers Ecol. Evol. 6, 149.
Sjögren, P., Edwards, M.E., Gielly, L., Langdon, C.T., Croudace, I.W., Merkel, M.K.F., Alsos, I.G., 2017. Lake sedimentary DNA accurately records 20th Century introductions of exotic conifers in Scotland. New Phytol. 213 (2), 929–941.
Skre, D., 1997. Raknehaugen. En empirisk loftsrydding. Viking 60, 7–42.
Soininen, E.M., Gauthier, G., Bilodeau, F., Berteaux, D., Gielly, L., Taberlet, P., Yoccoz, N.G., 2015. Highly overlapping winter diet in two sympatric lemming species revealed by DNA metabarcoding. PloS One 10 (1), e0115335. https://doi.org/10.1371/journal.pone.0115335.
Solberg, B., 2000. *Jernalderen i Norge: ca. 500 f. Kr.-1030 e. Kr.* Cappelen akademisk forlag.
Solheim, S., Persson, P., 2018. Early and mid-Holocene coastal settlement and demography in southeastern Norway: comparing distribution of radiocarbon dates and shoreline-dated sites, 8500–2000 cal. BCE. J. Archaeol. Sci.: Report 19, 334–343. https://doi.org/10.1016/j.jasrep.2018.03.007.
Solheim, S., Iversen, F., 2019. The mid-6th century crises and their impacts on human activity and settlements in southeastern Norway. Ruralia 423–434.
Soltvedt, E.C., Henningsmoen, K.E., 2016. Agricultural and household activities in Vestfold, Southeast Norway, as illustrated by pollen data and the charred remains of crops and wild plants. Environ. Archaeol. 21 (1), 11–30.
Sønstebø, J.H., Gielly, L., Brysting, A.K., Elven, R., Edwards, M., Haile, J., Brochmann, C., 2010. Using next-generation sequencing for molecular reconstruction of past Arctic vegetation and climate. Mol. Ecol. Res. 10 (6), 1009–1018. https://doi.org/10.1111/j.1755-0998.2010.02855.x.
Sørensen, L., Karg, S., 2014. The expansion of agrarian societies towards the north—new evidence for agriculture during the Mesolithic/Neolithic transition in Southern Scandinavia. J. Archaeol. Sci. 51, 98–114. https://doi.org/10.1016/j.jas.2012.08.042.
Stephens, L., Fuller, D., Boivin, N., Rick, T., Gauthier, N., Kay, A., Ellis, E., 2019. Archaeological assessment reveals Earth's early transformation through land use. Science 365 (6456), 897–902. https://doi.org/10.1126/science.aax1192.
Stockmarr, J.A., 1971. Tabletes with spores used in absolute pollen analysis. Pollen Spores 13, 615–621.

Støren, E.W.N., Paasche, Ø., Hirt, A.M., Kumari, M., 2016. Magnetic and geochemical signatures of flood layers in a lake system. Geochem., Geophys., Geosyst. 17 (10), 4236–4253. https://doi.org/10.1002/2016GC006540.

Sugita, S., 1994. Pollen representation of vegetation in Quaternary sediments: theory and method in patchy vegetation. J. Ecol. 881–897.

Sugita, S., Gaillard, M.J., Broström, A., 1999. Landscape openness and pollen records: a simulation approach. Holocene 9 (4), 409–421.

Taberlet, P., Coissac, E., Pompanon, F., Gielly, L., Miquel, C., Valentini, A., et al., 2007. Power and limitations of the chloroplast trn L (UAA) intron for plant DNA barcoding. Nucleic Acids Res. 35 (3). https://doi.org/10.1093/nar/gkl938 e14-e14.

Universitetsmuseenes samlingsportaler, 2020. UniMus: Universitetsmuseenes Samlingsportaler. http://www.unimus.no.

Vitousek, P.M., Mooney, H.A., Lubchenco, J., Melillo, J.M., 1997. Human domination of Earth's ecosystems. Science 277 (5325), 494–499.

Voldstad, L.H., Alsos, I.G., Farnsworth, W.R., Heintzman, P.D., Håkansson, L., Kjellman, S.E., Eidesen, P.B., 2020. A complete Holocene lake sediment ancient DNA record reveals long-standing high Arctic plant diversity hotspot in northern Svalbard. Quat. Sci. Rev. 234, 106207. https://doi.org/10.1016/j.quascirev.2020.106207.

Wanner, H., Solomina, O., Grosjean, M., Ritz, S.P., Jetel, M., 2011. Structure and origin of Holocene cold events. Quat. Sci. Rev. 30 (21–22), 3109–3123.

Warden, L., Moros, M., Neumann, T., Shennan, S., Timpson, A., Manning, K., Damsté, J.S., 2017. Climate induced human demographic and cultural change in northern Europe during the mid-Holocene. Sci. Rep. 7 (1), 1–11. https://doi.org/10.1038/s41598-017-14353-5.

Wieckowska-Lüth, M., Kirleis, W., Doerfler, W., 2017. Holocene history of landscape development in the catchment of Lake Skogstjern, southeastern Norway, based on a high-resolution multi-proxy record. Holocene 27 (12), 1928–1947. https://doi.org/10.1177/0959683617715691.

Wieckowska-Lüth, M., Solheim, S., Schülke, A., Kirleis, W., 2018. Towards a refined understanding of the use of coastal zones in the Mesolithic: new investigations on human–environment interactions in Telemark, southeastern Norway. J. Archaeol. Sci.: Report 17, 839–851. https://doi.org/10.1016/j.jasrep.2017.12.045.

Willerslev, E., Davison, J., Moora, M., Zobel, M., Coissac, E., Edwards, M.E., Taberlet, P., 2014. Fifty thousand years of Arctic vegetation and megafaunal diet. Nature 506 (7486), 47–51. https://doi.org/10.1038/nature12921.

Williams, M., Zalasiewicz, J., Haff, P.K., Schwägerl, C., Barnosky, A.D., Ellis, E.C., 2015. The anthropocene biosphere. Anthropocene Rev. 2 (3), 196–219.

Wood, S., 2018. Mixed GAM Computation Vehicle with GCV/AIC/REML Smoothness Estimation and GAMMs by REML/PQL. *R Package Version*, pp. 1–8.

Woodward, F.I., Lomas, M.R., Kelly, C.K., 2004. Global climate and the distribution of plant biomes. Phil. Trans. Roy. Soc. Lond. B Biol. Sci. 359 (1450), 1465–1476.